RHEOLOGY OF GAS-SOLID FLUIDIZED SYSTEMS

A THESIS

Presented to

the Faculty of the Graduate Division

by

Frank Fa-Keh Liu

In Partial Fulfillment

of the Requirements for the Degree

Master of Science

in Chemical Engineering

Georgia Institute of Technology

September, 1959

RHEOLOGY OF GAS-FLUIDIZED SYSTEMS

Approved:

_____

_____

_____

Date Approved by Chairman:

September 29, 1959

ACKNOWLEDGMENTS

TABLE OF CONTENTS

NOMENCLATURE

Letters

A_t	cross-sectional area of fluidization vessel, ft^2
C	conversion factor of spindle
d	deviation from Newtonian behavior, dimensionless
D	distance from air-distributor, <u>in</u>.
D_p	particle diameter, microns
f.r.	volumetric flow rate of gas, cc/min
G	mass flow rate of gas, lb/ft^2 hr
g	gravity force, ft/sec^2
g_c	gravitational conversion factor, lb_f ft/lb_m sec^2
L	height of the bed, ft
M_{Fr}	modified Froude number, dimensionless
$\triangle p$	pressure drop across the bed, <u>in</u>. of water
r	radius of fluidization vessel, <u>in</u>.
V_t	volume of bed, ft^3
W_b	bed weight, gm
μ	gas viscosity, centipoise
η	bed viscosity, centipoise
ρ_f	fluid density, lb/ft^3
ρ_p	particle density, lb/ft^3
λ	shape factor of particles, dimensionless

δ porosity of bed, dimensionless

τ shear stress (viscometer reading), arbitrary unit

LIST OF TABLES

LIST OF FIGURES

SUMMARY

In recent years, fluidization techniques have become widely used in industry. The reasons for industry's acceptance lie primarily in two unique characteristics of fluidized systems, namely, their convenience for carrying out mass transfer operations and their efficient heat transfer. Many other applications of the fluidization technique are still being investigated.

Due to the complexity of gas-solid fluidized systems, an understanding of the fundamental factors controlling their behavior is required if most efficient use is to be made of the technique. A major deterent in the advancement of fundamental knowledge in gas-solid fluidization is the lack of a comprehensive index of the quality of fluidization occurring in a given apparatus, most experimental investigations having been confined to the study of gross phenomena. Very few studies of local phenomena within fluidized beds have been reported, although a few workers have attempted to use X-ray and capacitive methods. From the liquid-like properties of gas-solid fluidized systems it would appear that viscosity might be employed to a greater extent than it has been in characterizing fluidization behavior. Detailed analysis of phenomena in fluidized beds by means of rheological properties has not previously been attempted, as far as this investigator is aware.

This investigation presents the use of apparent viscosity as a qualitative tool for the study of local phenomena within a fluidized bed.

Experiments were conducted using four groups of glass beads with different average diameters, one group of silica alumina cracking catalyst, and one group of polystyrene beads. Mass flow rates of air between six and one-hundred pound per square foot per hour were employed with a fluidized bed that was 1.75 in. in diameter and up to about 18 in. in height. Viscosity measurements were made at various points within the fluidized section from one inch above the distributor (bottom) to two inches from the surface of the bed. Temperature, humidity, minor vibration, and wall effects were neglected. A viscometer manufactured by the Brookfield Engineering Laboratories, Inc., Stoughton, Mass., and described as a synchro-lectric, model LVF, was used with a modified spindle in measuring viscosity. When the spindle was inserted in the fluidized bed it produced no visible disturbance and apparently did not affect the fluidization.

It was found that the section of the fluidized bed composing approximately the lowest ten per cent of the bed (for beds not less than seven inches in depth) had viscosity properties as reported by previous workers, and that the viscosity decreased with increasing flow rate and increased with increasing particle size. However, for other sections of the bed such viscosity relations were not applicable. While measurements made at any point along a fluidized bed would indicate viscosity to be a function of particle size, particle density, bed weight, and gas flow rate, no comparision of data can be made unless the point of measurement is specified.

It was also found that at low flow rates apparent viscosity decreases with an increase in bed height, while at high flow rate it

increases with the bed height. In the section of bed extending from approximately twenty per cent above to twenty per cent below the midpoint of the bed, viscosity changes only slightly as flow rate changes. This section may be referred to as a transition region. Transition phenomena have also been found by others when making capacitive, porosity measurement. It should also be pointed out that the change of viscosity with the flow rate at various positions along the bed gave characteristic relationships corresponding to porosity distributions as reported by other workers. From shear diagrams it appears that zero shear stress is attained at zero shear rate in all cases. The diagrams show also that Newtonian behavior sometimes extends to relatively high shear rates.

The results of this investigation show that viscosity measurements can be used at least as a qualitative tool to study local phenomena within a variety of different types of gas-solid fluidized beds.

CHAPTER I

INTRODUCTION

Fluidization techniques and uses have developed rapidly in recent years. Both liquid-solid and gas-solid systems are now widely used. Although considerable research has been conducted on both systems, many problems remain that require further study.

Most of the experimental investigations of gas-solid fluidized system have been confined to a study of gross phenomena, such as total pressure drop, conditions for fluidization, and the like. Grohse (1) and Bakker and Heertjes (2) have, however, used X-ray and capacitive methods to study local phenomena within the fluidized bed. They succeeded in obtaining an analysis of the density and the porosity distribution along a bed, but their methods required complicated and very sensitive instruments. In the capacitive method, moreover, the experiment was restricted to certain types of materials.

Because of the liquid-like properties of a gas-solid fluidized system, it appeared that a measure of viscosity probably could be made to characterize the behavior of a fluidized bed even though only a few such rheological studies have ever been attempted. Matheson, et al., (3) and Ohmae and Furukawa (4) used a Stormer viscometer fitted with a paddle as ordinarily employed with liquids to measure the viscosity of a fluidized system the solid component of which consisted of cracking catalyst and

polyvinyl acetate particles. Their results showed that viscosity decreased with increasing gas flow rates, and increased with increasing particle size. The rotation of their paddle undoubtedly created a stirring action that resulted in a contraction of the fluidized bed. This action may in some cases have caused enough disturbance to destroy the characteristic flow pattern of the particles in the fluidized bed. Since the gas-solid fluidized system is usually a non-Newtonian and compressible, interpreting viscosity data obtained with an apparatus ordinarily used to measure liquid systems is difficult at best and generally impossible. Diekman and Forsythe (6) used a Brookfield viscometer (Brookfield Engineering Laboratories, Inc., Stoughton, Mass.) with a spindle made of screen wire to measure the viscosity of a gas-solid fluidized bed of cracking catalyst particles. Their results also showed that viscosity decreases with increasing gas flow rates. However, in their system the bed height was kept constant by drawing away the overflow when the flow rate was increased. Furthermore all viscosity measurements were made at one fixed point in the bed, the macroscopic particle distribution in the different sections of the bed not being taken into consideration. Since the gas passing through a bed expands as it nears the top, bed properties are different in different sections, and one viscosity measurement at one point cannot define the properties of the entire bed. It is true, however, that a measurement made at any one point of a bed would indicate viscosity to be a direct function of particle size, particle density, bed weight, and gas flow rate. It is

clear that no comparision of data can be made unless the point of measurement is specified.

A modified viscosity probe was developed in this work to measure the viscosity of gas-solid fluidized systems; its use creates a mimimum of disturbance within the bed. Viscosity measurements were also made at various points of the bed. The viscosities determined in this study show qualitatively and quantitatively the relation between viscosity and particle size, density, bed weight, and gas flow rate in different sections of beds of several materials.

A series of measurements was made using six groups of particles with different sizes and densities. Mean values of viscosity were determined, and correlations were made involving viscosity, mass flow rate of gas, particle diameter, particle density, and bed weight.

CHAPTER II

THEORETICAL BACKGROUND AND DESCRIPTION OF PHENOMENA

When a fine, granular material is placed in a vessel the mass reveals a finite bulk density. This bulk density depends, in part, on the size and shape of the particles. When an upward stream of gas is passed through a supported and laterally-confined mass of solid particles, reproducible changes in physical behaviour are observed which go through successive stages as the fluid velocity is increased. If gas is admitted at a very slow rate through a distributor into the bottom of the bed, a small pressure drop is indicated by a manometer. Leva, et al., (7) have derived the following equation for estimating the pressure drop Δp across a bed of particles through which a fluid is flowing under laminar conditions

$$\Delta p = \frac{200 \, L \, G \, \lambda^2 (1 - \delta)^2 \mu}{D_p^2 \, \rho_f \, g_c \, \delta^3} \tag{1}$$

Where G is the mass flow rate of the gas, μ is the gas viscosity, L is the bed height, λ is the particle shape factor, δ is the bed porosity, D_p is the particle diameter, ρ_f is the fluid density, and g_c is the gravitational conversion factor.

As the mass flow rate of gas is gradually increased, the pressure drop rises to a point at which the weight of the bed equals the pressure

drop across the column multiplied by the cross-sectional area of the vessel. Mathematically, this situation may be expressed by the simple relationship

$$\Delta P = \frac{V_t}{A_t} (1 - \delta)(\rho_p - \rho_f) \tag{2}$$

Where V_t is the volume of the bed solids, A_t is the cross-sectional area of the bed, ρ_p is the solid particle density, and other terms are as used previously. This relation was verified by Wilhelm and Kwauk (8), Parent, et al. (9), as well as by Leva, et al. (7). When the superficial gas velocity is just sufficient to support the particles the condition is one of "incipient fluidization". At this point a slight increase in fluid velocity causes an expansion of the bed and creates the "dense fluid" state in which the bed particles rest more upon a cushion of the fluid than directly upon each other. As the flow rate increases further the expansion of the bed reaches a maximum height. This maximum height depends on the particle size and density. The change in the bed porosity between the static bed and the fully fluidized bed can be calculated from

$$\delta = \frac{V_t - W_b/\rho_p}{V_t} \tag{3}$$

Where W_b is the weight of the bed, and other terms are as used previously.

From equations (1) and (2) it is possible to calculate the mass flow rate of fluid necessary to expand a static bed. For this Leva, et

al. (7) give the expression

$$G = \frac{0.05 \, D_p^2 \, \delta^3 \, (\rho_p - \rho_f) \, \rho_f \, g_c}{\lambda^2 \, (1 - \delta)} \qquad (4)$$

where all terms have been previously defined.

After the maximum height of the bed is reached, any further increase in flow rate has almost no effect on bed height and pressure drop. This type of bed is called an "aggregated fluidized bed". Such a system is composed of two phases, a continuous phase, consisting of uniformly distributed particles in a supporting gas stream, and a discontinuous phase, consisting of essentially solids-free gas, the latter passing through the bed in the form of bubbles. Single, continuous-phase fluidization remains stable until the maximum bed height is reached, and then any additional gas flow passes through the bed in the form of a discontinuous phase. As the discontinuous phase forms at the gas inlet, it is acted upon by a buoyant force due to its immersion in the denser phase, and thus it imparts convective motion to the continuous phase to produce "aggregative" fluidization. The amount and size of the discontinuous phase (i.e., the bubbles) depends on the gas mass flow rate, particle size and density, the weight of the bed, and also the type of gas distributor used in the system. Gas bubbles pass through a bed of small-size solids of good fluidity in a manner analogous to the upward flow of gas through a liquid of low viscosity. On the other hand, gas bubbles pass through a bed of coarse solids in a manner similar to gas passing through a viscous liquid. The liquid-like properties of the gas-

solid fluidized system have been discussed in many articles, such as
Ohmae and Furukawa's (5) article on "Liquid-like Properties of Fluidized
Systems".

When the bed is not expanded greatly by an increased gas velocity
there is considerable turbulence in the bed and more energy is lost in
inelastic collisions between particles. The degree of the turbulent
motion in a fluidized system depends primarily on the amount and size of
the discontinuous phase (i.e., the bubble size) passing through the bed.
The size of the discontinuous phase increases as it rises in much the
manner of a gas bubble rising through a vertical column of liquid. At
low flow rates particle movement is not entirely random. Particles can
be observed to rise through the center of the bed where the fluid velocity
is high and to fall at the walls of the vessel where the fluid velocity
is at a minimum. The particles near the discontinuous phase move upward
with this phase through the center of the column while other portions of
the continuous phase move downward. There is thus a constant top-to-
bottom turnover in the bed making it impossible to predict the location
of a particular particle at any time.

At high flow rates the discontinuous phase (i.e., bubbles) rises
spontaneously across the entire cross-section of the bed in large quan-
tities and sizes. The bubbles often combine to form larger bubbles while
rising from the bottom. The interaction of the two phases becomes more
vivid at this stage, and the particle movement becomes entirely random.
The behavior of rising bubbles is more obvious in beds of particles

having high densities and large diameters than it is in those of finer and lighter particles. A violent disturbance occurs when a large bubble bursts upon reaching the surface of a bed, particles often being thrown from the bed container if small equipment is being used.

At high flow rates a large number of bubbles, the discontinuous phase, is formed, and their size increases with bed height due to two effects as noted previously, namely, (1) pressure exerted on the bubble decreases with increased bed height causing the bubble to expand, and (2) combination of bubbles along the rising path. This increase in the size of the discontinuous phase was found to cause the voidage in the continuous phase to decrease and to produce high density at the interface *as well as in the continuous phase. As a result it increased the amount* of shear exerted on the measuring instrument.

CHAPTER III

DESCRIPTION OF APPARATUS

A plastic tube 1.75 in. in inside diameter and 18.5 in. in length was fitted tightly into a base flange to form the retaining vessel or fluidized-bed container. A piece of fine, strong cloth stretched across its lowest edge formed an air distributor as well as a support for the static bed. Pressure drop across the bed was measured with a U-tube manometer using water as the manometric fluid, one leg of the manometer being connected to the fluidized-bed vessel below the gas distributor and the other open to the atmosphere. Air flow rates were established using U-tube manometers and an orifice calibrated with a standard gas-meter. The measured pressure drop thus included that produced by the apparatus distributor as well as that across the bed of particles. However, the pressure drop caused by the distributor was essentially negligible. The general arrangement of the apparatus with its auxiliary equipment is shown in Figure 1. Figure 2 presents a photographic view of the apparatus.

A model LVF, synchro-lectric viscometer manufactured by Brookfield Engineering Laboratories, Inc., Stoughton, Mass., was used with a modified spindle for viscosity measurement. The spindle was specially designed; it consisted essentially of two thin hollow cylinders concentrically mounted as shown in Figure 3. In the Brookfield device the torque

1   Manometer No.1
2   Manometer No.2
3   Manometer No.3
4   Brookfield Viscometer
5   Plastic Column
6   Modified Spindle
7   Adjustable Arm
8   Adjustable Arm
9   Base Flange
10   Three-Way Valve
11   Pressure Gauge
12   Dust Protector
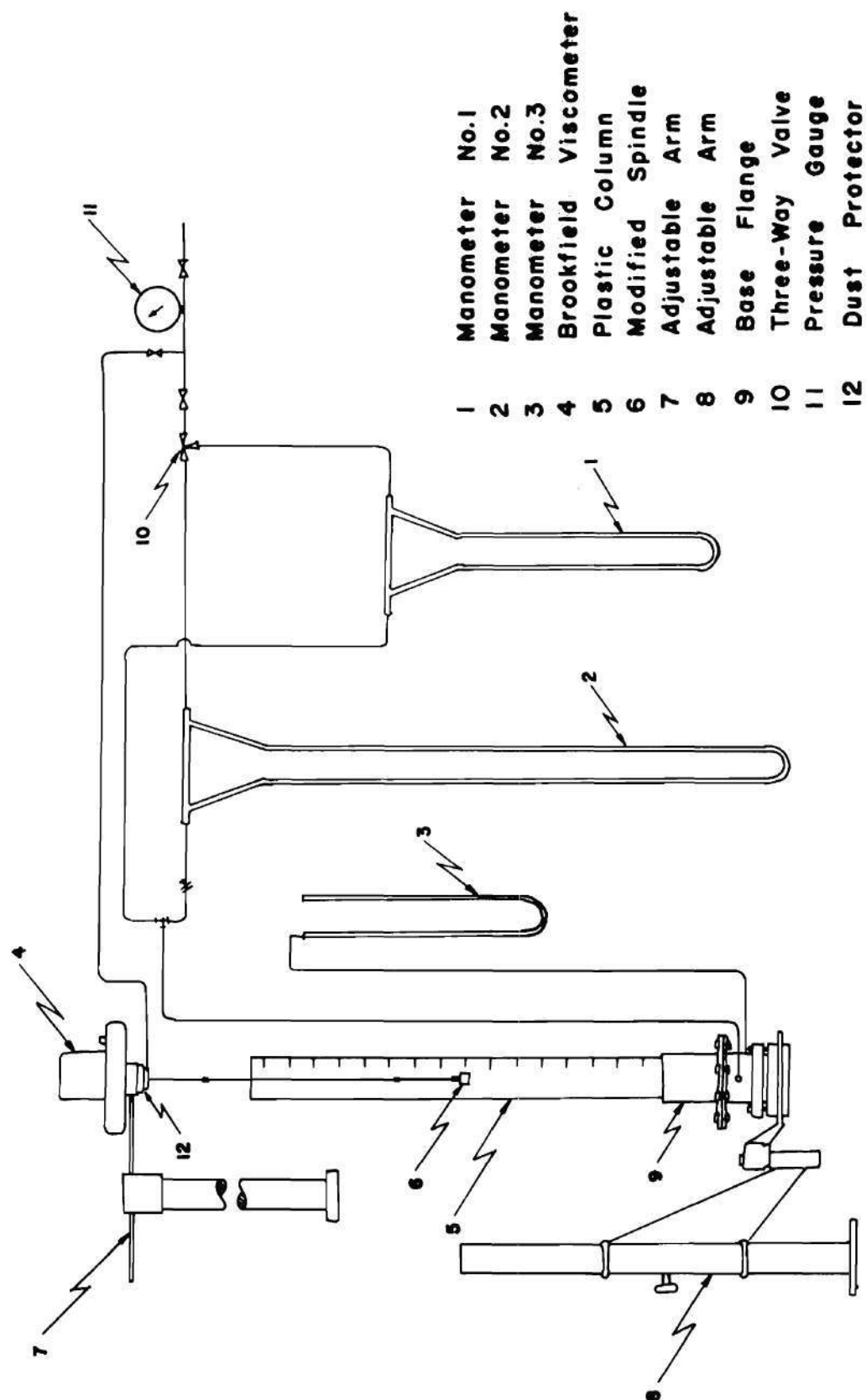
Figure 1. Schematic Arrangement of Apparatus.
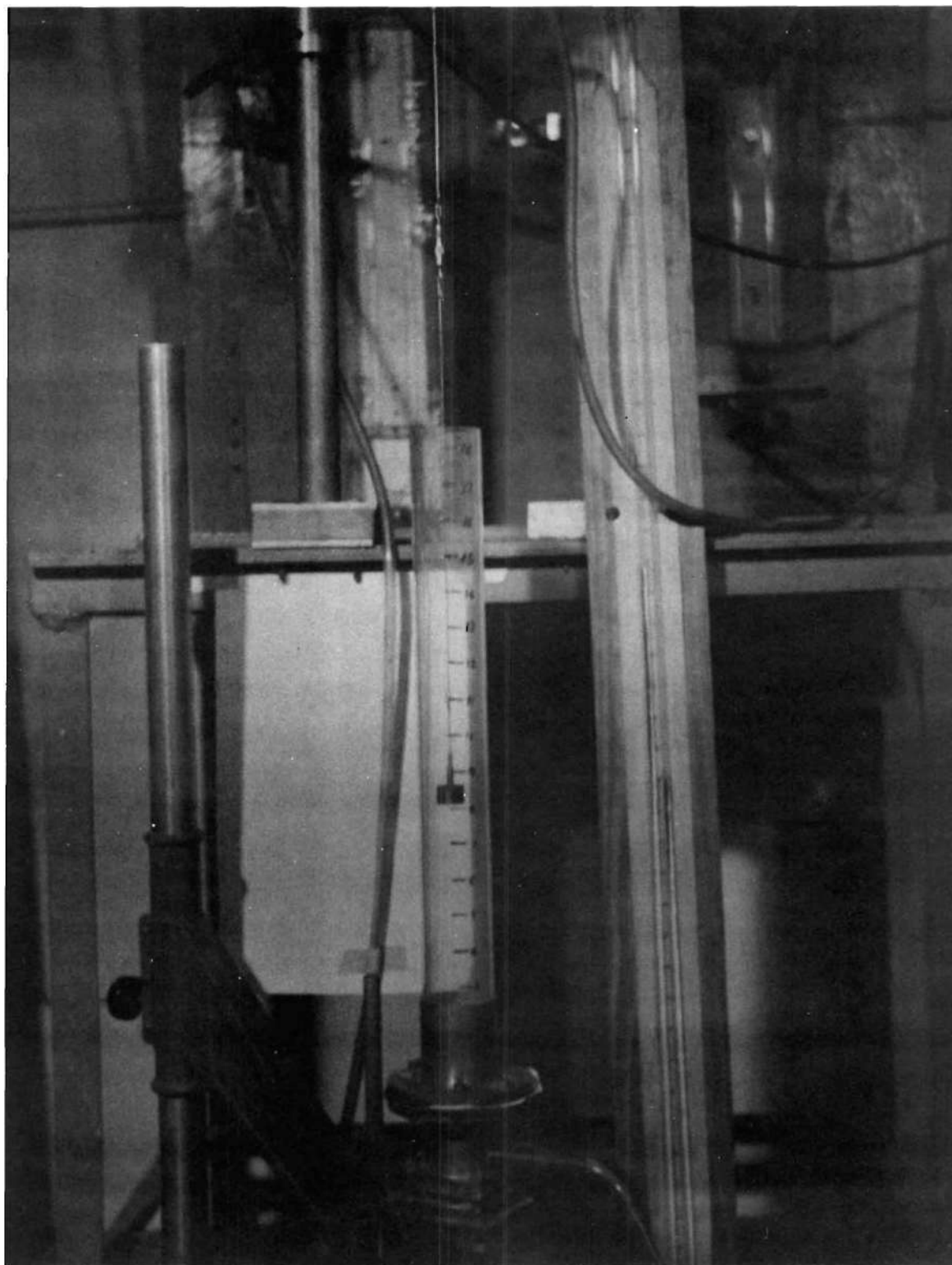
Figure 2. Photograph of Apparatus Showing Primarily the
Fluidized-Bed Column.
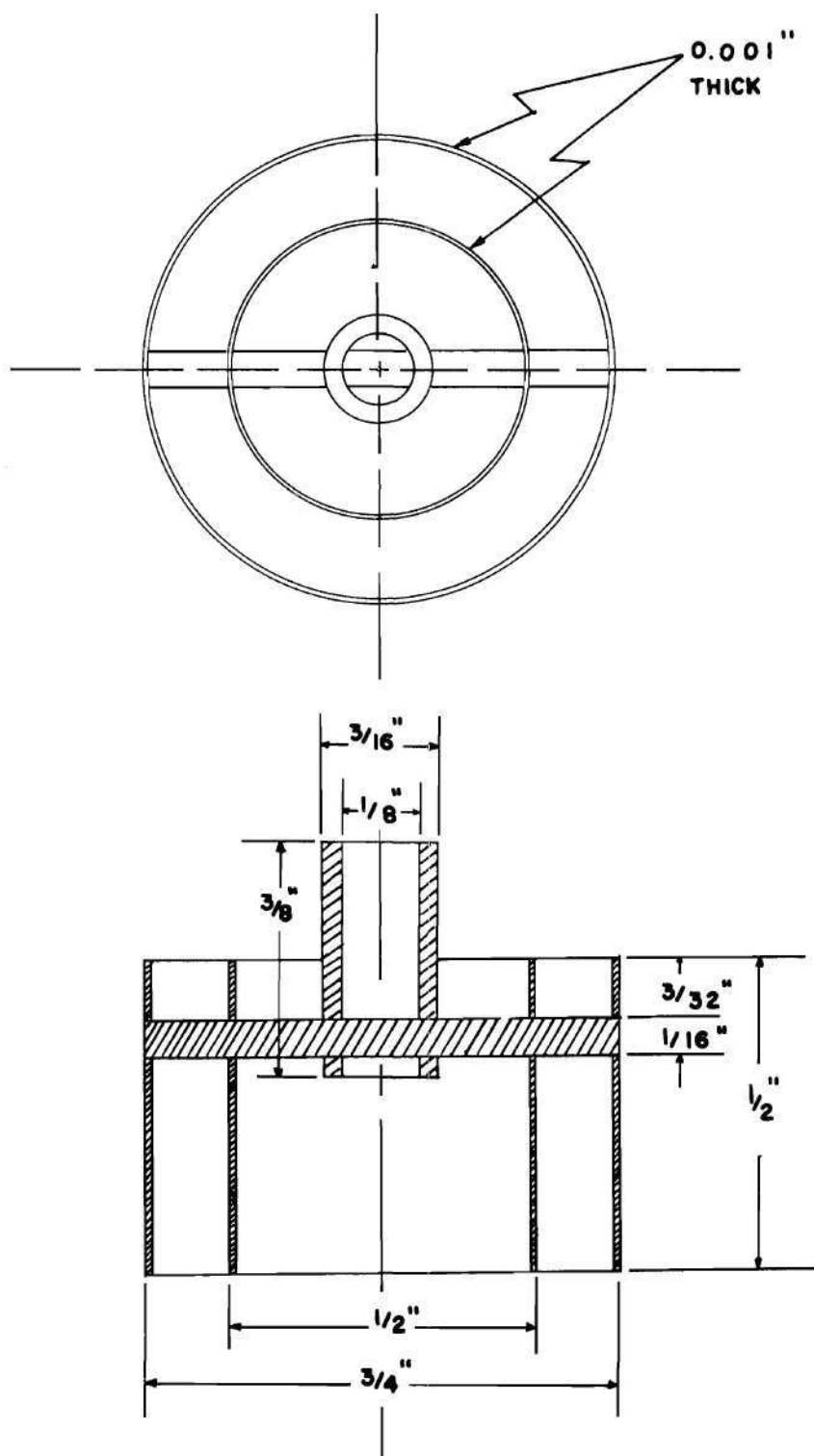
Figure 3. Design of Viscometer Spindle.

required for rotating the spindle is controlled by the displacement of a torsion spring and is translated directly to a dial reading on an arbitrary scale of 0 to 100. The viscometer may be operated at any one of four rotational speed and for each speed an equivalent viscosity constant must be determined in order to convert scale readings to viscosities. A Newtonian fluid, glycerol, was used to calibrate the viscometer. The resulting conversion factors are given in Table 1.

Table 1. Conversion Factor of Spindles

Viscometer Rotation Rate (rpm)	Conversion Factor[a]	
	Spindle No. 2[b]	Modified Spindle
6	50	35
12	25	17.5
30	10	7
60	5	3.5

[a]Conversion factor times viscometer reading equals viscosity in centipoise.

[b]Supplied by manufacturer.

The modified spindle was composed of two hollow cylinders with 0.001 inch thick walls of brass and different diameters. The one with the smaller diameter was supported within the large one, and both were held in place by a single small rod, the rod being welded through the walls of both cylinders. Plastic models were used during construction

to align the cylinders and rod. A small chuck was attached to the supporting rod to permit connection between the spindle and the main shaft of the viscometer.

Because of its unique design, the modified spindle, when inserted in a fluidized bed, offered an almost negligible area in the direction of movement of the gas stream. Even when rotating it retained its very small area of exposure. Occasionally the spindle oscillated a little because of the random flow pattern of the discontinuous phase, but this did not produce a sufficient disturbance to affect materially the upflow of particles in the gas stream. Due to the large surface area of the spindle exposed parallel to the path of gas stream, the instrument was, however, quite sensitive to changes in the viscous properties of the system. It may be pointed out also that the presence of the modified spindle in the fluidized bed produced no tendency to contract the bed, whereas the paddle type spindle commonly used with the Stormer viscometer does produce such a contraction. There is no indication that this method of measurement must be restricted to the experimental materials used here. The arrangement of the experimental apparatus and auxiliary equipment should provide a convenient method for analyzing other local phenomena in fluidized beds.

CHAPTER IV

EXPERIMENTAL MATERIALS

Pertinent information for the materials fluidized is given in Table 2.

Table 2. Descriptive Data for Experimental Materials

| Material | Density (gm/cc) | Particle Size | | Method of Measurement |
		Range of Diameters (μ)	Median Diameter (μ)	
Glass beads[a];				
Group A	2.47	115-163	123	Microscopic count
Group B	2.47	90-120	99	Microscopic count
Group C	2.47	73-111	88	Microscopic count
Group D	2.47	21-79	44	Micromerograph[b]
Silica Alumina Cracking Catalyst[c]	2.12	2-62	45	Micromerograph
Polystyrene beads[d]	1.05	280-550	349	Microscopic count

[a]Product of Minnesota Mining and Manufacturing Co., Minneapolis, Minn.

[b]A device utilizing air sedimentation that is manufactured by the Sharples Corp., Philadelphia, Pa.

[c]Product of Davison Chemical Co., Baltimore, Md.

[d]Type 8X, product of Tennessee Eastman Co., Kingsport, Tenn.

Median particle diameters were obtained from a logarithmic-probability plot of the cumulative weight per cent of particles finer than a given size <u>versus</u> that size; on such a plot the 50 per cent size is also the median size. Table 4 in the Appendix gives the complete size distribution of each material.

CHAPTER V

EXPERIMENTAL PROCEDURE

Air from a regulated supply at a constant pressure of 20 psia and having a relative humidity of approximately 15 per cent was used to produce fluidization. The particles to be used were weighed and carefully transferred into the fluidization vessel. In order to prevent electrostatic charges being built-up by friction between the particles and the wall of the vessel during the filling of the vessel, the particles were transferred through a paper tube. For polystyrene particles, a very small amount of fine carbon powder (approximately 0.2 per cent by weight) was added to the batch to reduce electrostatic effects; the carbon worked, apparently, by increasing the bed conductivity. An approximate bulk density for the bed was calculated from the observed bed height.

To start the fluidization, air was admitted at increasing rates into the system. The gas flow rate and pressure drop required for reaching the incipient fluidization point and the point of maximum bed height was set by observation, the vessel wall being of plastic. From this initial observation a check with the previously calculated values from Leva's equation was made in order to assure that the system was operating correctly. A leak in the system or some other difficulty was easily detected by comparing the observed values with calculated ones.

After the initial start-up period, the flow rate was increased to the turbulent stage for the bed and held at that point for a short time. This put all particles in motion, and left no dead section in any part of the bed. The flow rate was then decreased to the desired rate and sufficient time was allowed for the bed to stabilize before any measurements were taken. Flow rate, pressure drop, and bed height were recorded after the bed reached its stabilized state. Then viscosity measurements were taken at different points in the bed, the point of measurement being based on the distance from the bottom air distributor. Due to the violence of the motion near the upper surface, measurements were not taken at less than two inches below the surface. After each change of spindle position in the bed, a short waiting period was necessary in order to let the bed establish a new equilibrium condition. With beds of fine particles especially, external vibrations were guarded against, because they have considerable effects of the stability of the bed. The spindle arm of the viscometer was always checked after each change of position in the bed to be sure it was at the center. Several measurements were recorded for each condition but mean values were used in later correlations.

The apparent viscosities obtained in this investigation were based on a given system of fixed column diameter, a particular type of gas distributor, and air as the fluidizing medium. The effects of temperature, humidity, minor vibration, and the nearness of the wall on viscosity measurements were neglected.

The rotational speed of the viscometer determines the shearing rate, and the torque indicated by the viscometer is the shearing stress.

When the viscometer reading is multiplied by the proper conversion factor as given in Table 1 for each rotation rate, apparent viscosities having units of centipoise are obtained.

For convenience of discussion, the terms "high" and "low" flow rate were used in this study, the condition being established in terms of a modified Froude number M_{Fr}, written

$$M_{Fr} = \frac{11 \, (f. \, r.)^2 \, \rho_f}{\pi^2 \, r^4 \, D_p \, g \, \rho_p} \tag{5}$$

where f. r. is the air flow rate, r is the radius of the fluidization vessel, and all other terms are as previously defined.

A system having a modified Froude number larger than 120 was considered to be in a condition of high flow rate, whereas less than 50 was taken to be a low flow rate. Between modified Froude numbers of 50 and 120 the condition was considered one of intermediate flow rate.

Due to the large size of polystyrene beads, its fluidization system required different limits of modified Froude numbers to describe low and high flow rates; they are, respectively, 200 and 500 for low and high flow rates.

Modified Froude numbers for different systems are tabulated in Table 3 and plotted in Figure 4.

Table 3. Modified Froude Number for

Various Solids as a Function of Flow Rate

| Flow Rate (cc/min) | Glass Beads | | | | Catalyst | Polystyrene |
	Group A	Group B	Group C	Group D		
660	7.7	9.68	10.78	21.6	24.6	---
1430	36.2	45.0	50.6	101.0	115.6	---
1910	64.4	80.1	90.0	180.0	206.0	---
2270	91.3	114.0	127.7	256.0	291.0	---
2550	115.0	143.0	161.0	322.0	369.0	95.0
3075	---	---	---	---	---	138.6
4450	---	---	---	---	---	290.0
5950	---	---	---	---	---	520.0
7575	---	---	---	---	---	841.0
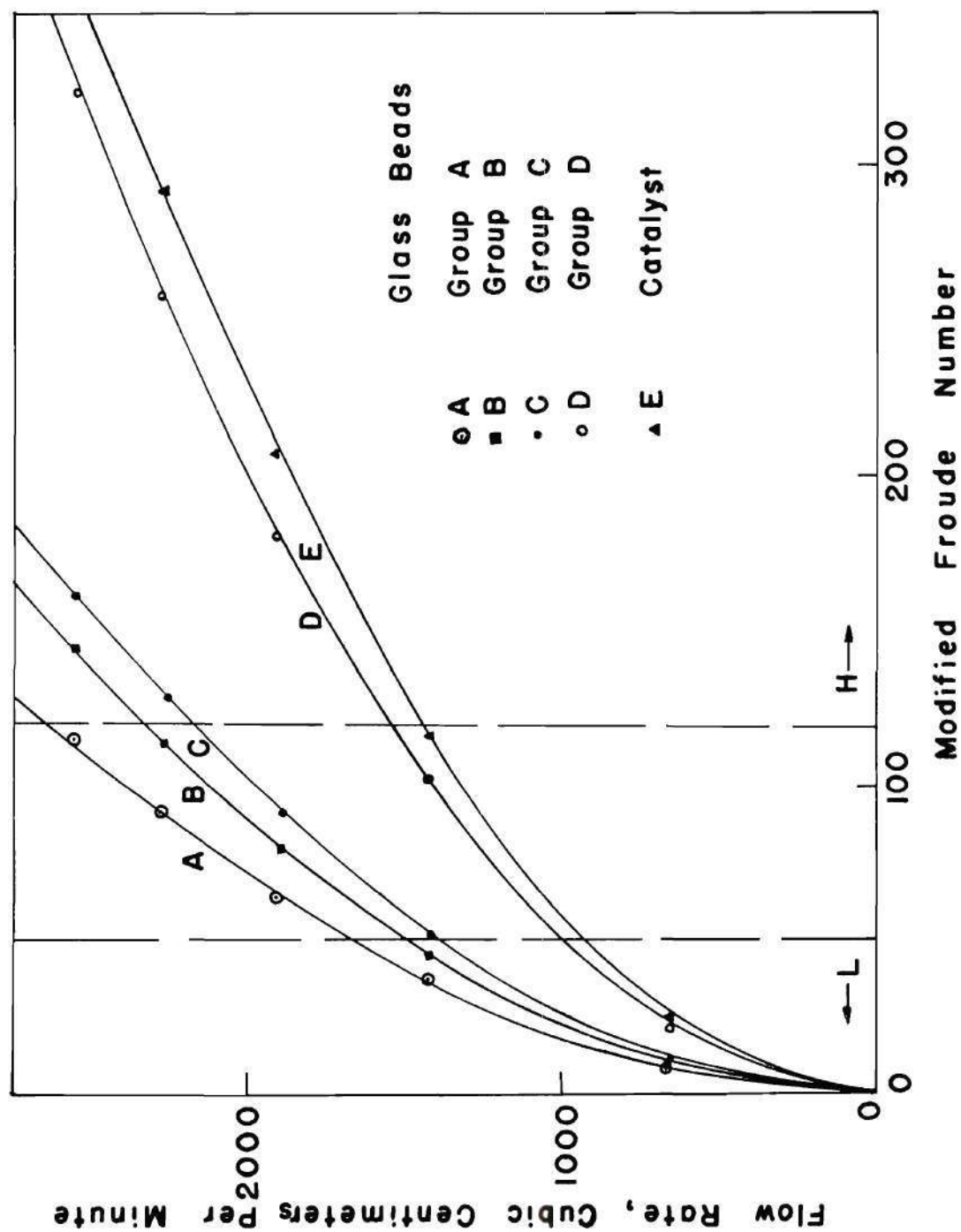
Figure 4. Flow Rate as a Function of Modified Froude Number for Various Fluidized Systems.

CHAPTER VI

EXPERIMENTAL RESULTS AND DISCUSSION

All experimental data are presented in tables in the Appendix.

Pressure drops across the different beds from static to fluidized conditions are shown in Figure 5, these data were checked by equations 1 and 2, given previously, and found to agree well with them. For the fixed bed region the relationship between pressure drop and flow rate was checked by equation 1, while for the fully fluidized bed the data were checked with equation 2. Disregarding kinetic and other external effects, the calculated pressure drops multiplied by the cross-sectional area of the vessel equaled the weight of the fluidized bed. As shown in Figure 5, the slope of the lower parts of the curves, i.e., in the fixed bed region, increases with decrease in particle size. The value of maximum pressure drop also increases with decrease of particles size.

Since the viscosity data obtained in these experiments are describing local phenomena within the fluidized bed and since each local section has been found to exhibit different characteristic response to the variables controlling fluidization, it is necessary to analyze the data sectionwise rather than as a whole. The following analysis of data is therefore based on three approximately equally-divided sections of the bed. Section I covers approximately the lower one-third of the fluidized bed height; section II is the center part of the bed; and section III is the upper one-third of the bed.
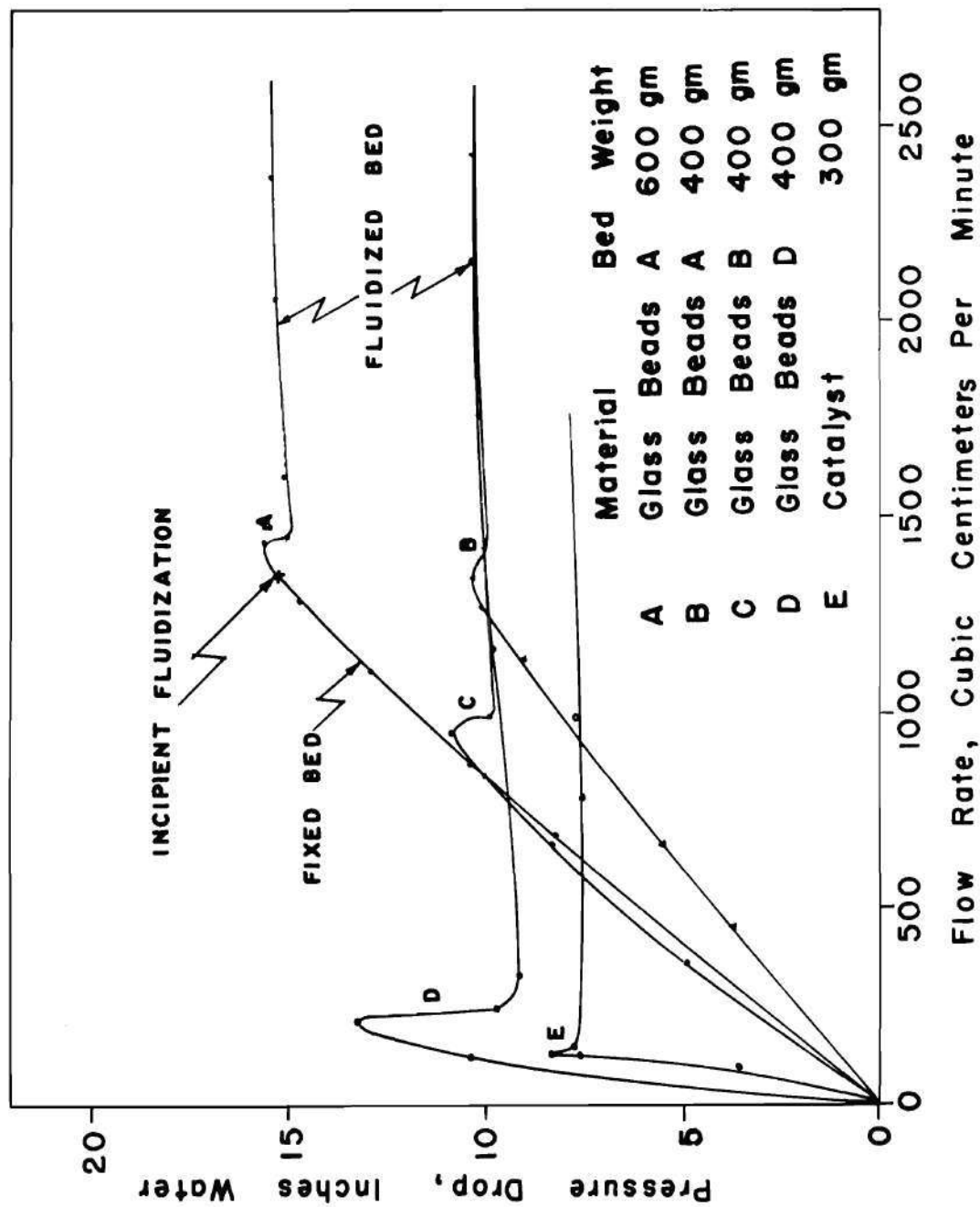
Figure 5. Pressure Drop Across the Fluidized Bed With Increasing Gas Flow Rate.

Phenomena in section I were found to be similar to occurrence reported by previous workers on the rheological properties of fluidized beds. For example, it has been reported that viscosity decreases with increasing flow rate and increases with increasing particle size. As shown by Figures 6 and 7, the data of this study for section I agree well with these reported characteristics. In addition, Figure 8 shows that viscosity increases with increasing bed weight in section I.

In section II, a transition region seems to exist in which viscosity is almost independent of flow rate. Figures 9, 10, 11, and 12 show the effect. The location of this transition region was found to vary for different conditions. The extent of the transition region, likewise, probably varies; it is smaller for coarser particles. Transition phenomena were also observed in Bakker and Heertjes' (2) capacitive porosity measurements.

For section III, Figures 9, 10, 11, 12, and 13 indicate that viscosity increases with increasing flow rate. The relation between viscosity and particle size or bed weight in section III is random and unpredictable as shown by Figures 7 and 8.

Four shearing rates were used in measuring the torque exerted on the viscometer spindle at fixed positions in the fluidized bed. The data so obtained make possible construction of a so-called shear diagram for the various sections of the bed. Such diagrams are presented in Figure 14. From them it can be seen that the gas-solid systems employed in this study behave as pseudoplastics at low flow rate and approach Newtonian

Material		Bed Weight
Glass Beads	B	400 gm
Glass Beads	D	400 gm
Catalyst		200 gm
Polystyrene		300 gm
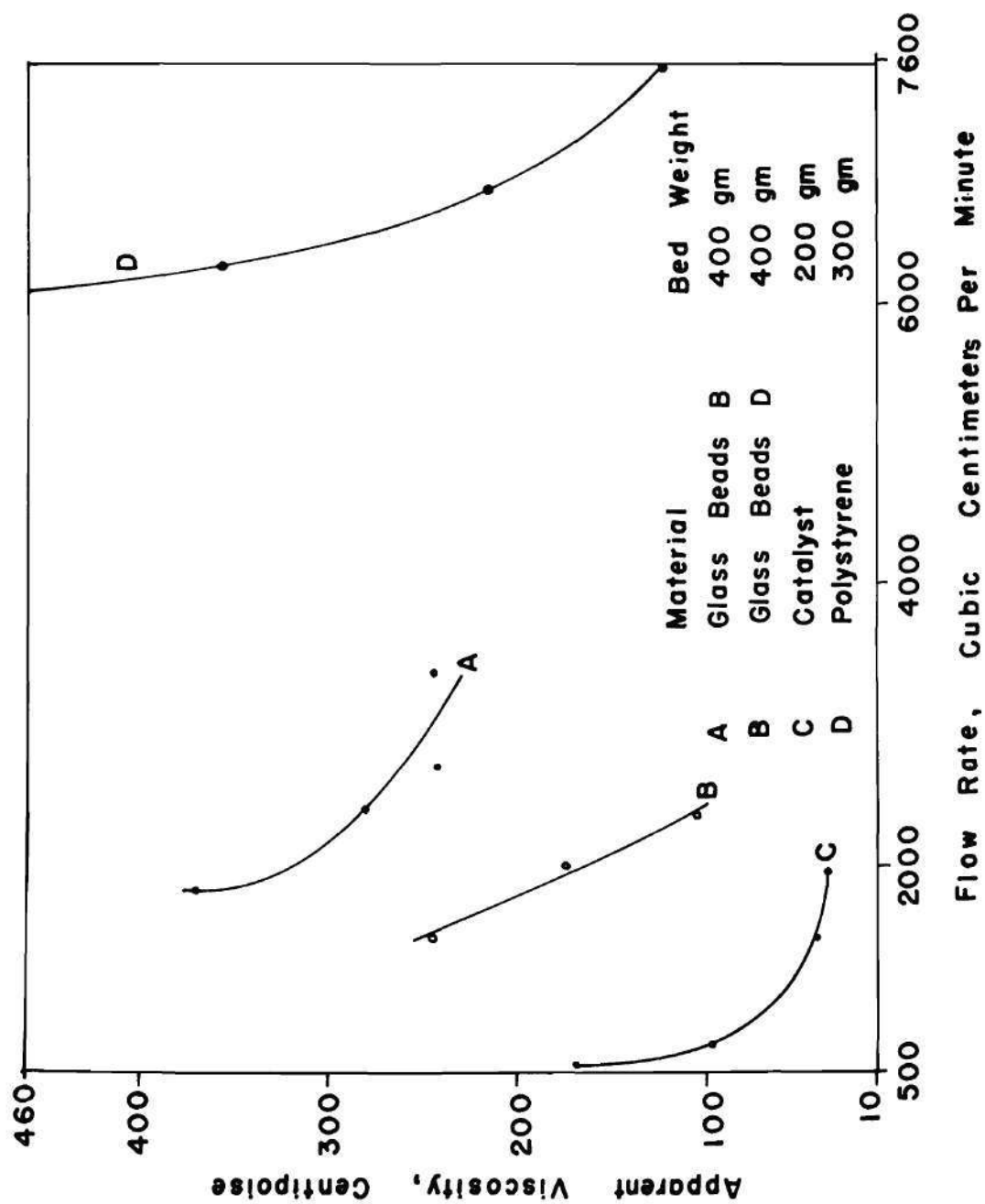
Figure 6. Change of Apparent Viscosity With Gas Flow Rate.
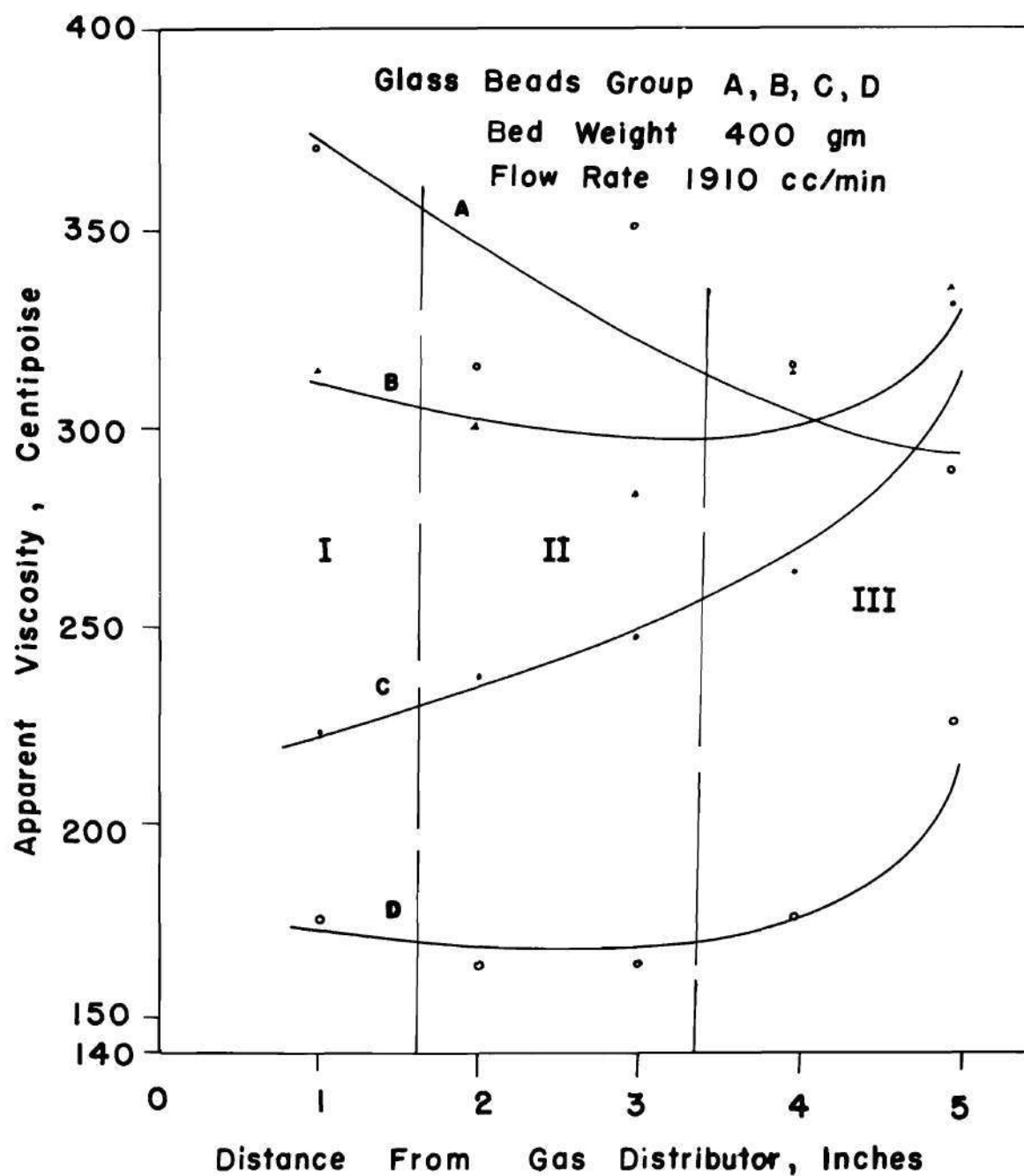
Figure 7. Change of Apparent Viscosity Within the Fluidized Bed.
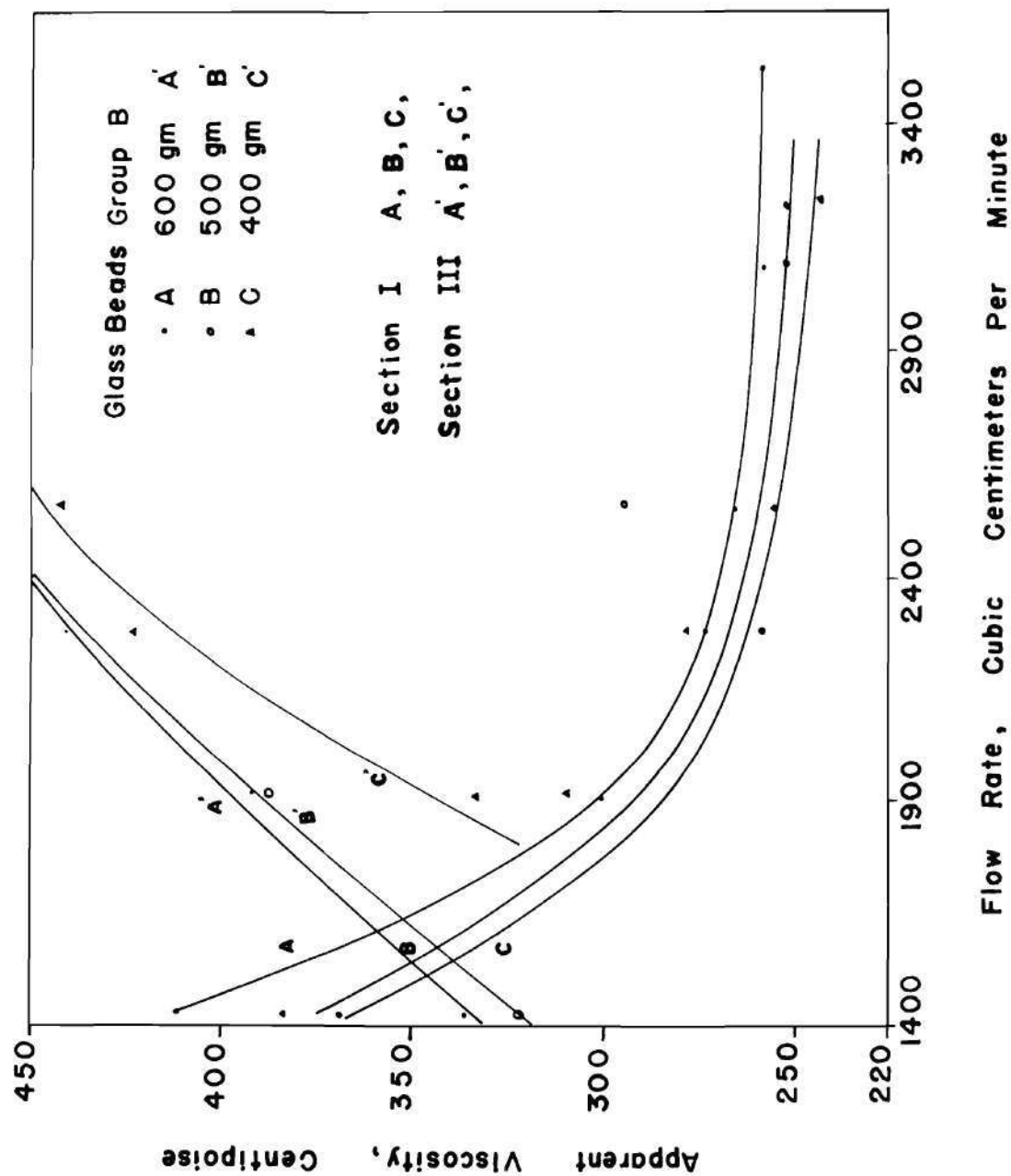
Figure 8. Change of Apparent Viscosity With Gas Flow Rate.
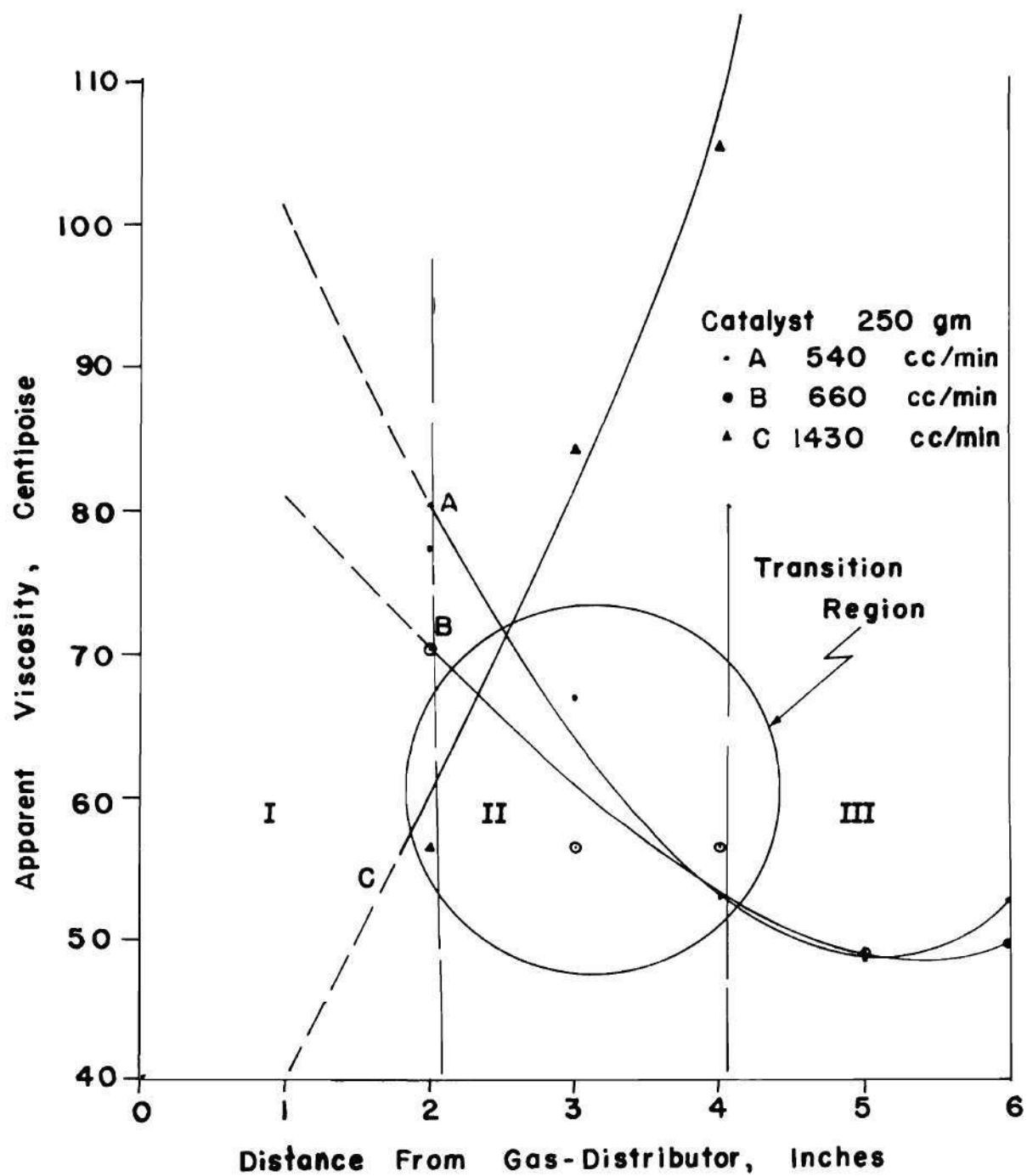
Figure 9. Change of Apparent Viscosity Within the Fluidized Bed.
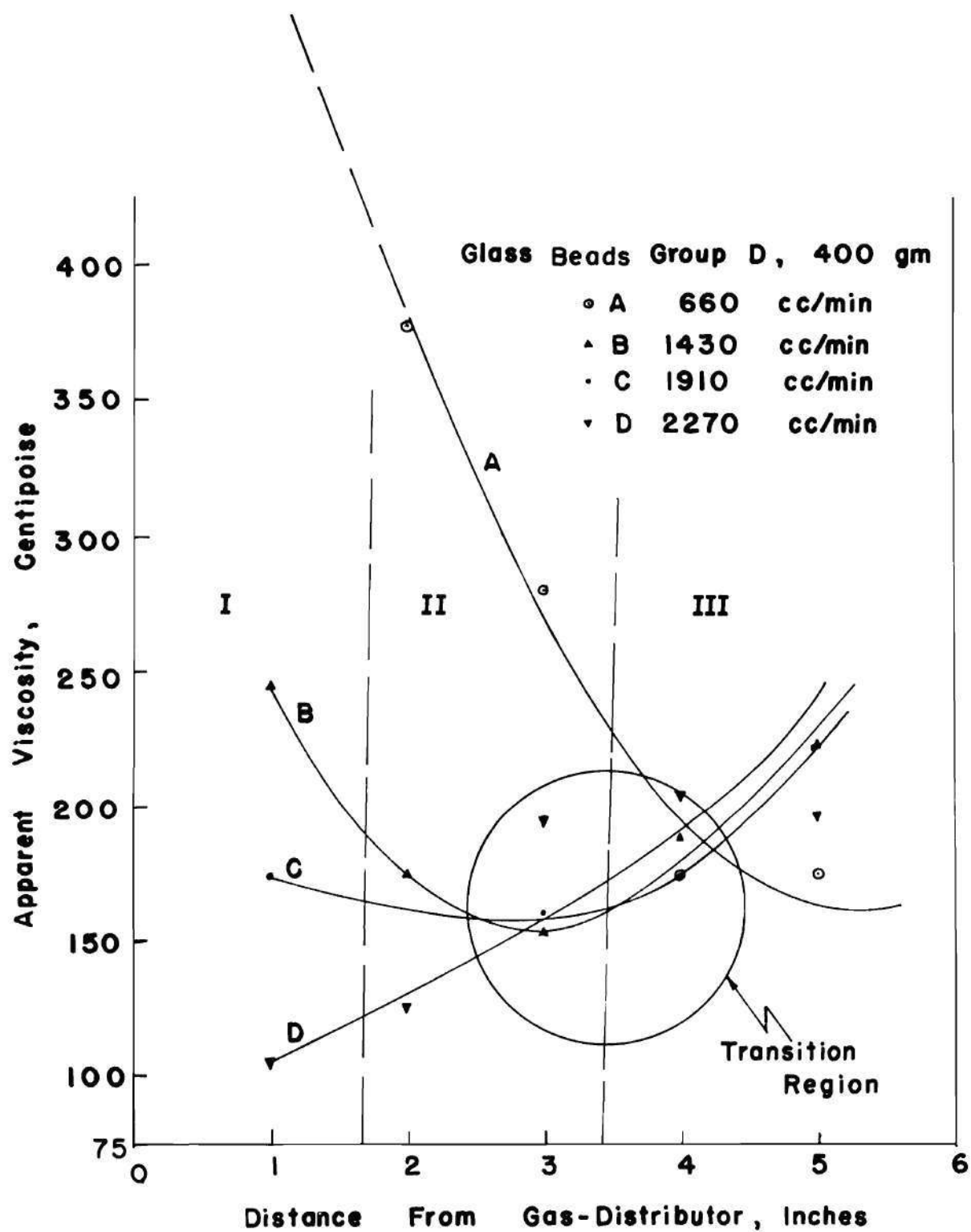
Figure 10. Change of Apparent Viscosity Within the Fluidized Bed.
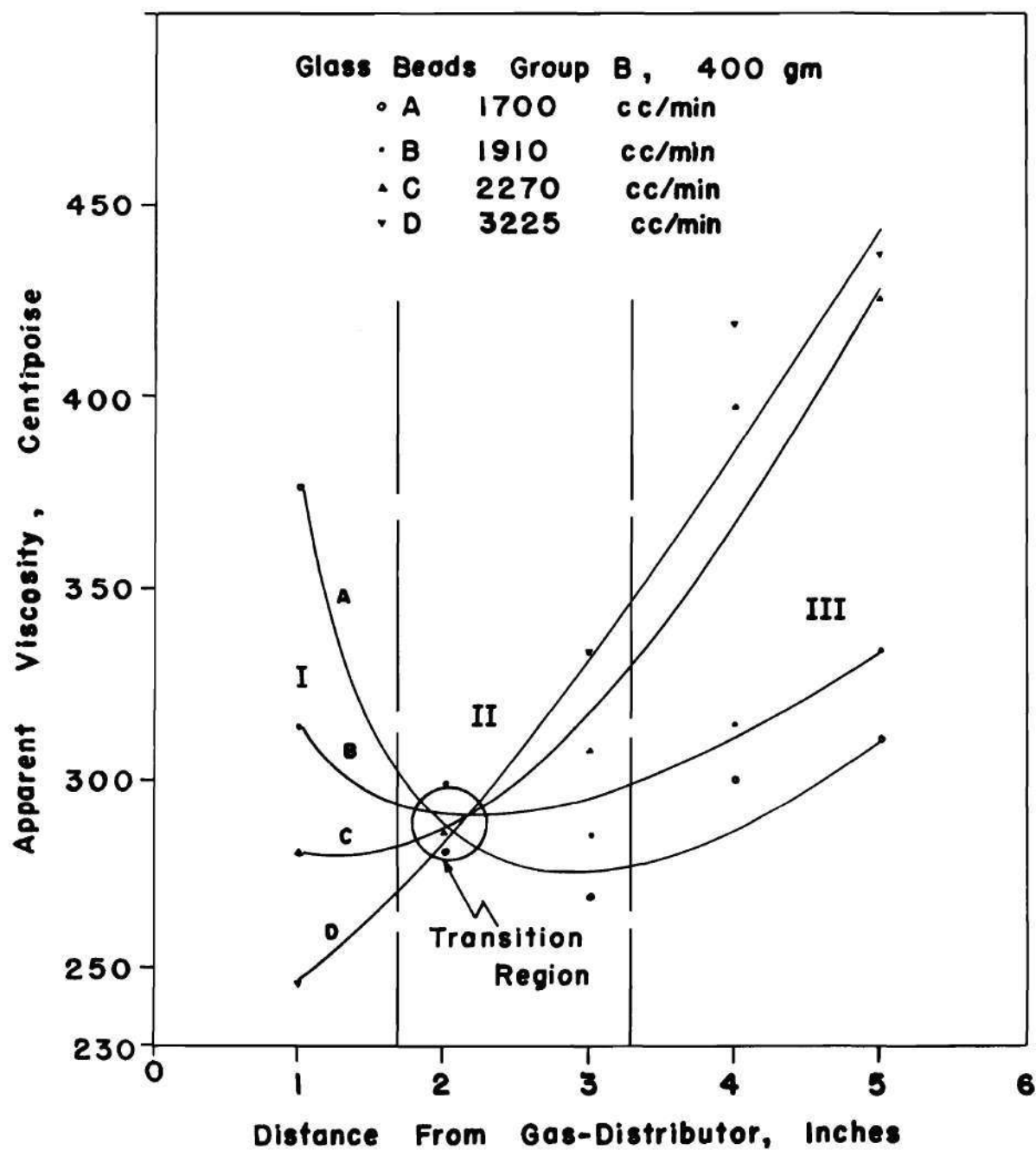
Figure 11. Change of Apparent Viscosity Within the Fluidized Bed.
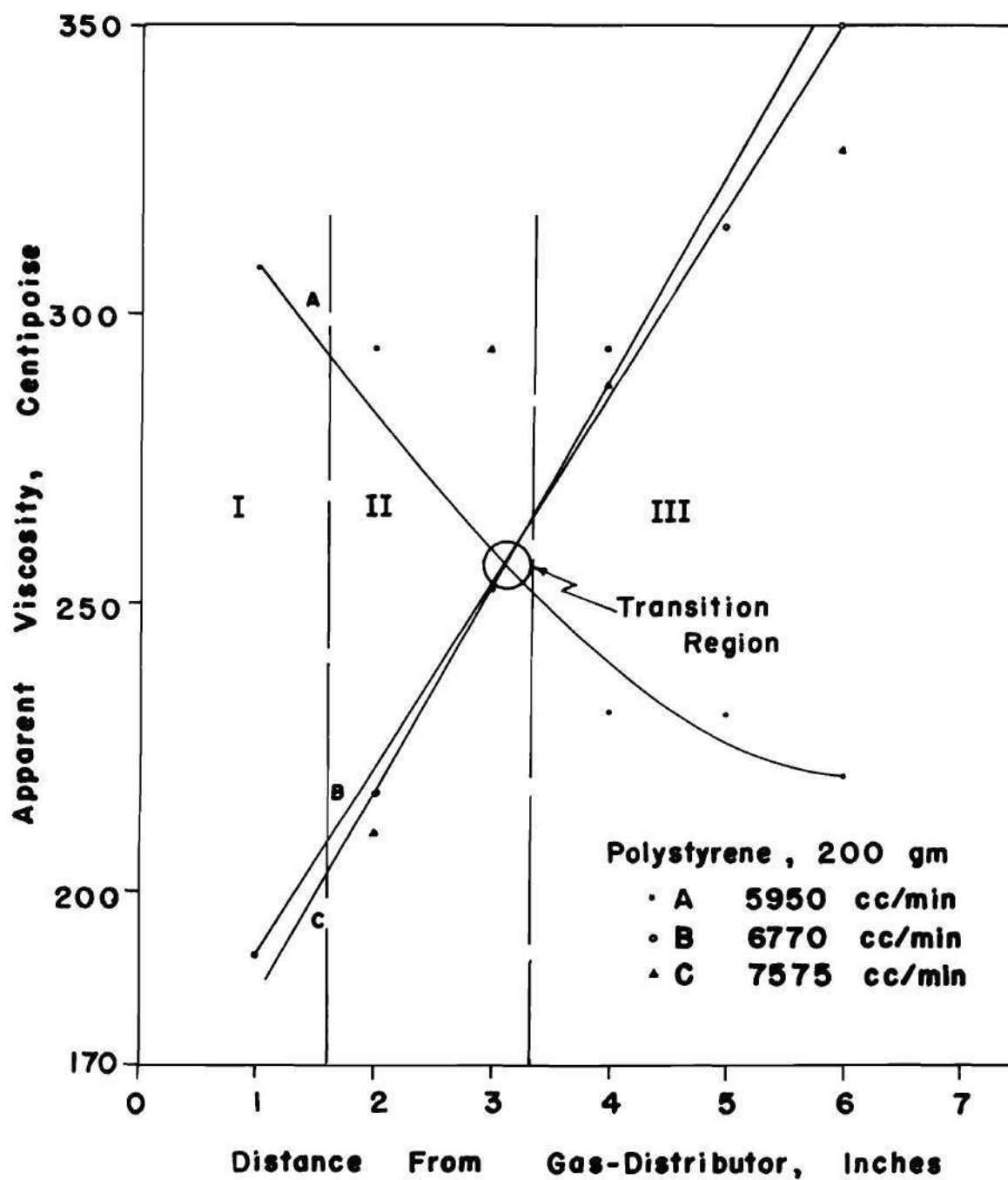
Figure 12. Change of Apparent Viscosity Within the Fluidized Bed.
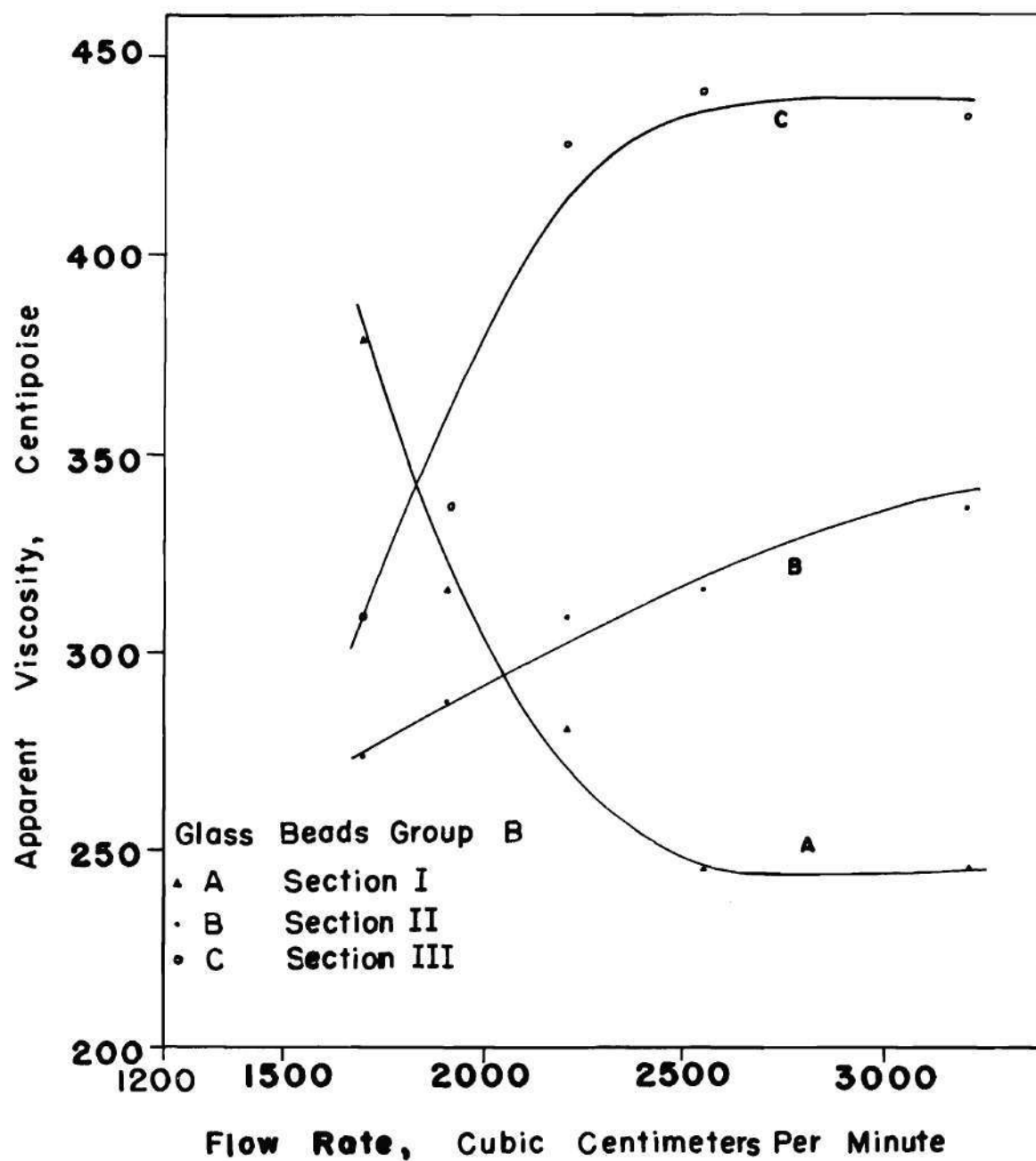
Figure 13. Change of Apparent Viscosity With Gas Flow Rate.
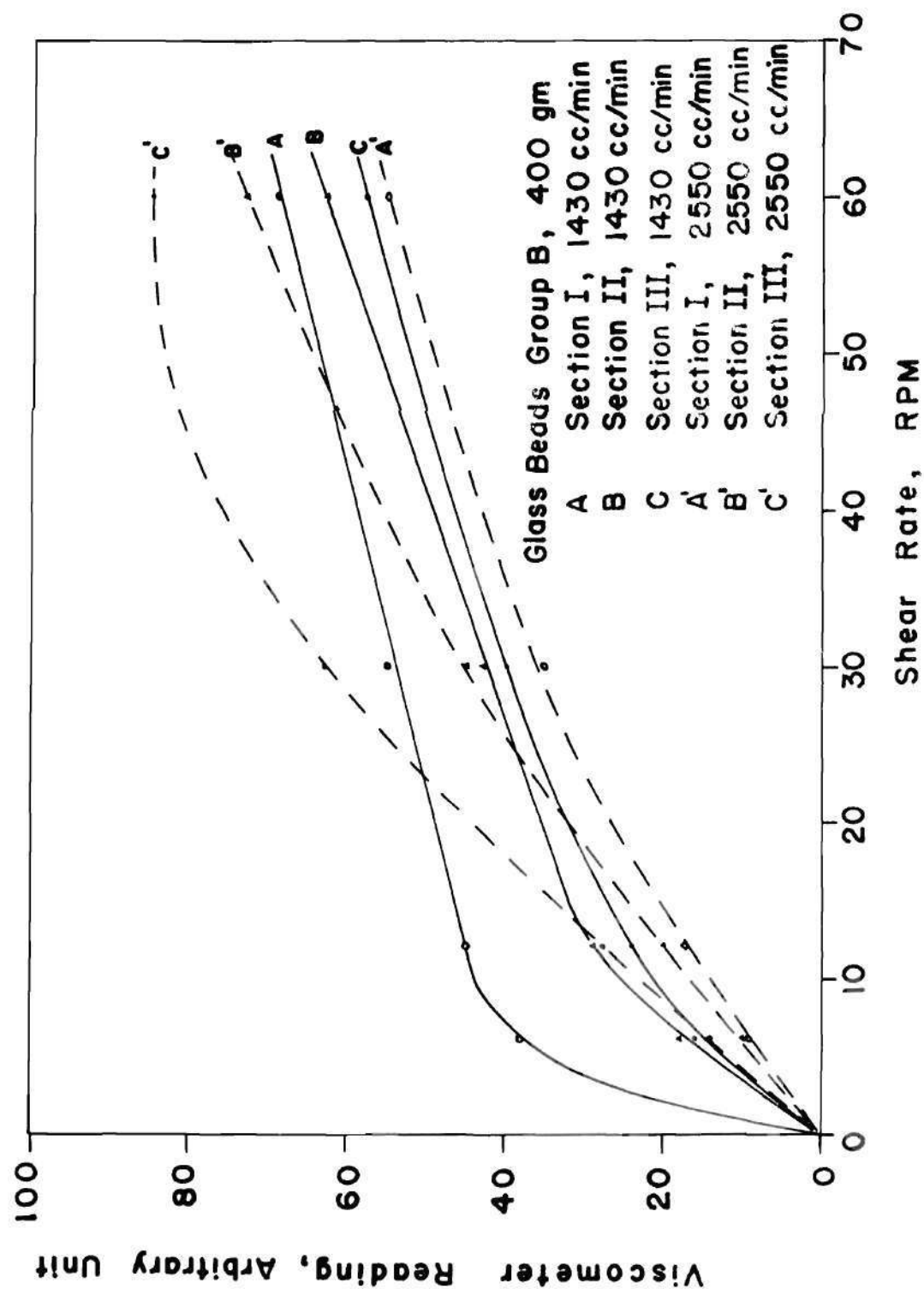
Figure 14. Shear Diagram.

behavior for the higher flow rates. All curves appear to exhibit zero shearing stress at zero shearing rate. No yield stress was evident for any system.

Figures 15 and 16 show that deviation from Newtonian behavior decreases as the flow rate increases. It has been suggested that the motion of high-velocity particles at conditions of high gas flow rate is analogous to the movement of molecules in a liquid. Ohmae and Furukawa (5) consider that interparticle forces analogous to intermolecular forces in liquids exist in the fluidized bed and that these may afford a possible explanation for the Newtonian behavior of a fluidized bed under certain conditions.

All data show a reproducibility of 80 to 95 per cent, the reproducibility being better in the case of the finer particles than with the coarser particles.
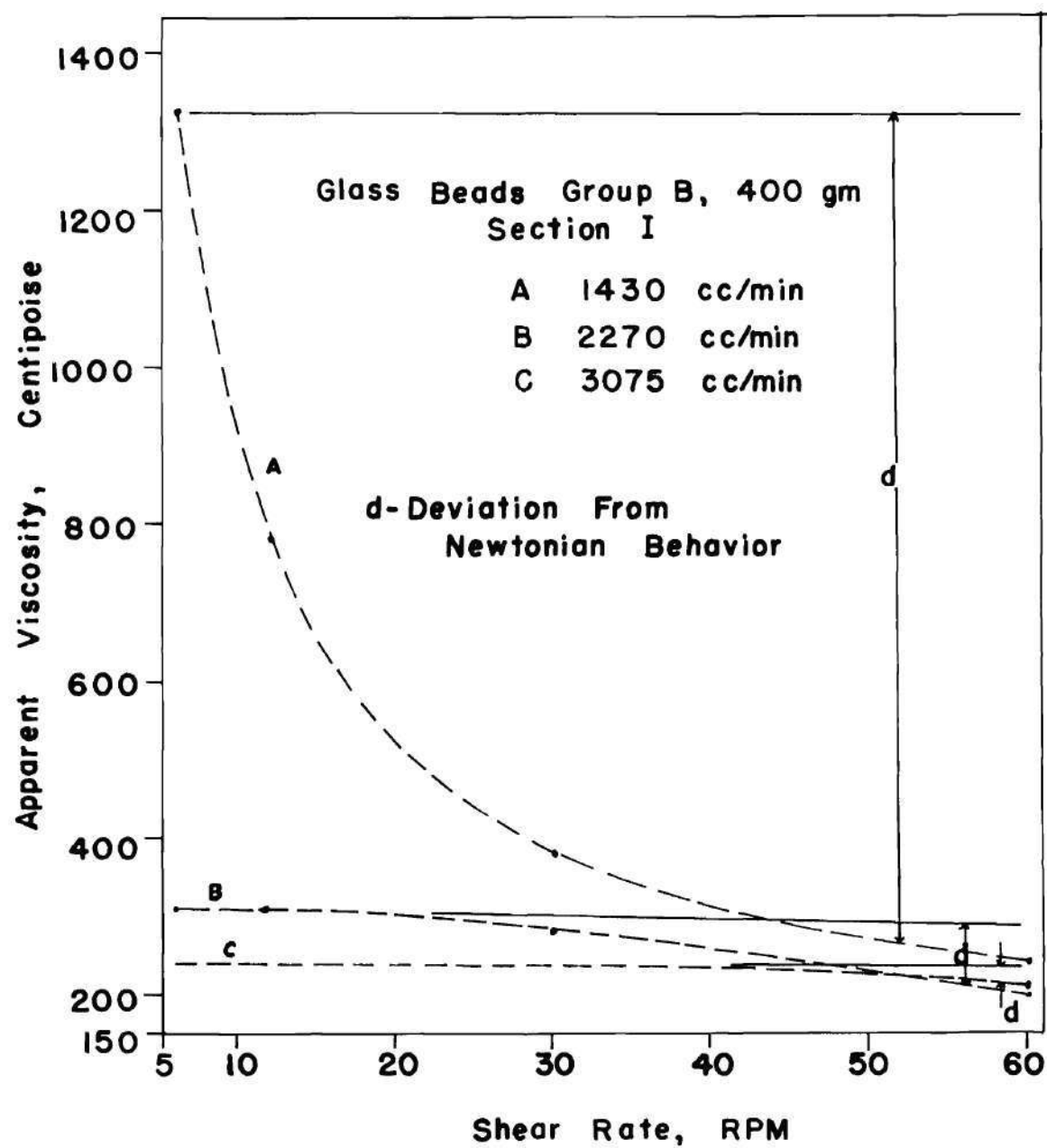
Figure 15. Deviations From Newtonian Behavior.
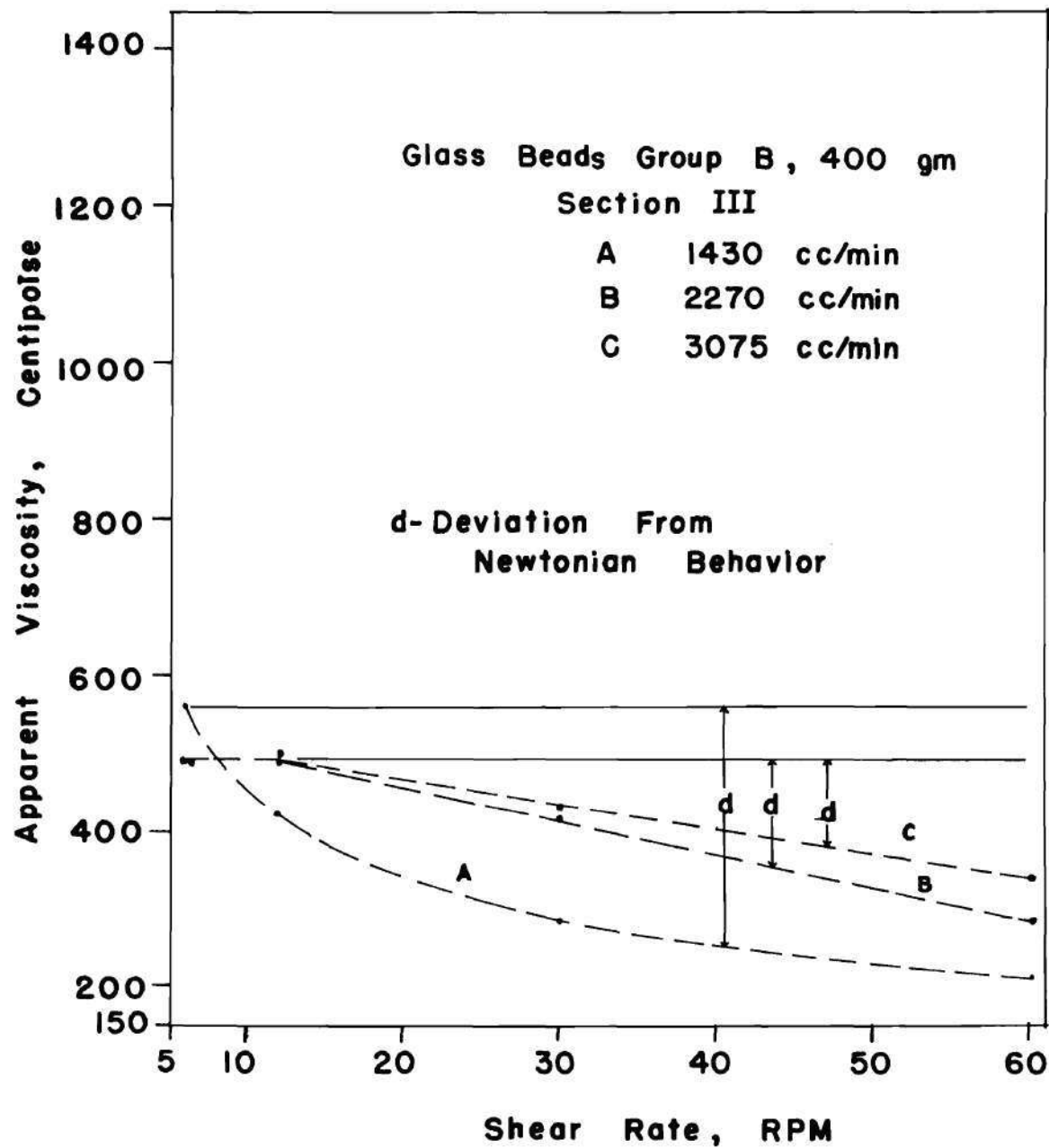
Figure 16. Deviations From Newtonian Behavior.

CHAPTER VII

CONCLUSIONS

From the results of this investigation it is concluded that:

1. The modified spindle used in these experiments is very useful and sensitive in measuring the viscosity of a gas-solid fluidized system. It makes available a convenient method for analyzing local phenomena in such a bed.

2. Sections of a gas-solid fluidized bed respond differently to changes of conditions within the system. As a result, it is necessary to characterize a bed by sections, i.e., by local phenomena. On the basis of three approximately equal sections, section I being that lowest part of the bed near the gas-distributor, section II the middle region of the bed, and section III the top protion, it was found for the conditions covered here that (a) in section I viscosity decreases with increasing flow rate, (b) in section III viscosity increases with increasing flow rate, (c) in sections I and II viscosity increases with increasing particle size, (d) in section III the relationship of viscosity with particle size is random, (e) in section I viscosity increases with increasing bed weight, while (f) in sections II and III this relationship is random.

3. A transition region near the middle of the bed exists in which viscosity changes only slightly with a wide change of flow rate. The

extent of the transition region decreases with an increase of particle size; its location in the bed varies somewhat with conditions of the system but mostly it is located near the central part of the bed.

4. Newtonian behavior for a fluidized bed exists under high gas flow rates. The theory of interparticle forces within a fluidized bed, by analogy with intermolecular forces of liquids, could be a possible explanation of the Newtonian behavior of fluidized beds at high flow rates.

CHAPTER VIII

SUGGESTIONS FOR FUTURE STUDY

This study has only been a preliminary one of local phenomena in a fluidized bed using rheological measurements. Many variables, such as the vessel size, type of gas, type of gas distributor, temperature, and humidity were held constant; any or all of these might be varied in some future investigation. The method presented might also be very useful for studying a binary system (a mixture of two groups of particles) composing a fluidized bed.

A data recording system attach to the viscometer as used in this work would enable a study to be made of time-dependent functions and also, by recording continuously, to obtain better values for viscosity.

APPENDIX

Table 4.   Size Distribution

(Measured by Microscope)
Polystyrene Bead Diameters

(μ)	(μ)	(μ)	(μ)
370	350	300	500
400	430	440	370
370	370	510	250
330	510	380	290
310	430	380	300
370	280	350	360
335	320	400	400
390	450	450	460
325	400	320	370
325	380	330	310
352	230	500	360
365	440	380	330
495	360	280	350
400	360	350	450
360	350	400	310
430	470	440	270
440	320	460	330
430	350	400	350
390	470	280	400

(Continued)

Table 4. Size Distribution (Continued)

(Measured by Microscope)
Polystyrene Bead Diameters

(μ)	(μ)	(μ)	(μ)
480	320	320	550
320	350	330	460
300	440	420	520
380	360	280	530

Average Value = 381μ
Microscope Factor = 0.916
Average Diameter of Particles = 381 x 0.916 = 349μ.

(Measured by Microscope)
Glass Beads, Group A

130	115	149	141
125	148	138	126
140	119	118	144
135	121	138	129
147	122	141	129
123	140	141	98
144	134	148	124
145	131	116	138
135	163	141	130
140	144	141	136
152	151	129	115

(Continued)

Table 4. Size Distribution (Continued)

(Measured by Microscope)
Glass Beads, Group A

| 135 | 140 | 135 | 136 |
| 124 | 137 | 94 | 132 |

Average Value = 133.6 μ
Microscope Factor = 0.916
Average Diameter of Particles = 133.6 x 0.916 = 123 μ.

(Measured by Microscope)
Glass Beads, Group B

116	111	112	106
103	98	105	108
98	108	106	108
115	108	114	104
106	100	90	113
114	116	120	118
106	111	119	120
115	96	122	101
98	114	91	120
117	110	98	98

Average Value = 107.8 μ
Microscope Factor = 0.916
Average Diameter of Particles = 107.8 x 0.916 = 99 μ.

(Continued)

Table 4.   Size Distribution (Continued)

(Measured by Microscope)
Glass Beads, Group C

96	94	96	102
100	100	93	103
98	98	96	102
83	99	97	94
102	103	98	101
100	91	100	99
80	96	93	92
100	93	102	98
102	111	83	104
95	94	102	85
80	96	91	103

Average Value = 96.02 μ
Microscope Factor = 0.916
Average Diameter of Particles = 96.02 x 0.916 = 88 μ.

(Measured by Micromerograph)
Glass Beads, Group D

Diameter of Beads (μ)	Percentage[a] (%)
76	100
57	87
48	60

(Continued)

Table 4. Size Distribution (Continued)

(Measured by Micromerograph)
Glass Beads, Group D

Diameter of Beads (μ)	Percentage[a] (%)
42	41
38	29
34	20
30	11
27	8
23	4
19	1
13	0

Median Diameter[b] = 44 μ.

[a]Weight percentage of beads finer than the micron size stated.

[b]Median diameter was obtained from a logarithmic probability plot of cumulative weight per cent finer than a given micron size; the median diameter was obtained as the micron size at the 50% point.

(Measured by Micromerograph)
Silica Alumina Cracking Catalyst

Diameter of Beads (μ)	Percentage[a] (%)
76	100.0
62	92.8

(Continued)

Table 4. Size Distribution (Concluded)

(Measured by Micromerograph)
Silica Alumina Cracking Catalyst

Diameter of Beads (μ)	Percentage[a] (%)
51	65.7
45	50.0
41	40.7
37	31.4
33	22.9
29	16.4
25	11.4
21	8.6
19	7.1
16	5.8
14	3.3
12	2.8
2	0

Median Diameter[b] = 45μ.

[a]Op. cit., page 44.

[b]Op. cit., page 44.

Table 5.   Pressure Drop Data

Glass Beads, G. A.; Bed Weight, 400 gm

Flow Rate (cc/min)	Pressure Drop (in. of water)
480	3.75
660	5.45
990	7.75
1130	9.0
1285	10.05
1370	10.35
1430	10.0
1635	10.1
2190	10.15
2485	10.15

Glass Beads, G. A.; Bed Weight, 500 gm

538	4.75
710	7.15
990	9.40
1251	11.85
1385	13.00
1430	12.45

(Continued)

Table 5. Pressure Drop Data (Continued)

Glass Beads, G. A.; Bed Weight, 500 gm

Flow Rate (cc/min)	Pressure Drop (in. of water)
1635	12.55
2060	12.70
2305	12.75
2665	12.85

Glass Beads, G. A.; Bed Weight, 600 gm

685	8.3
850	10.0
1110	12.85
1290	14.75
1350	15.30
1430	15.60
1450	15.0
1635	15.10
2060	15.25
2380	15.40
2680	15.40

(Continued)

Table 5. Pressure Drop Data (Continued)

Glass Beads, G. B.; Bed Weight, 400 gm

Flow Rate (cc/min)	Pressure Drop (in. of water)
355	4.90
480	6.10
660	8.25
870	10.4
950	10.95
990	9.85
1400	10.05
1740	10.10
2060	10.15
2320	10.20
2600	10.25

Glass Beads, G. B.; Bed Weight, 500 gm

Flow Rate (cc/min)	Pressure Drop (in. of water)
355	5.55
660	8.85
710	10.30
805	12.15
910	13.2
1010	13.40

(Continued)

Table 5. Pressure Drop Data (Continued)

Glass Beads, G. B.; Bed Weight, 500 gm

Flow Rate (cc/min)	Pressure Drop (in. of water)
1185	12.45
1505	12.60
1960	12.65
2320	12.70
2700	12.70

Glass Beads, G. B.; Bed Weight, 600 gm

250	5.45
615	11.30
805	14.45
935	16.05
1030	16.15
1070	15.00
1510	15.15
1765	15.30
2160	15.30
2460	15.35

(Continued)

Table 5. Pressure Drop Data (Continued)

Glass Beads, G. C.; Bed Weight, 400 gm

Flow Rate (cc/min)	Pressure Drop (in. of water)
325	5.1
536	8.1
640	10.1
685	10.4
690	9.7
830	9.8
1370	10.1
1755	10.1
2380	10.2
2660	10.25

Glass Beads, G. C.; Bed Weight, 500 gm

240	5.1
425	8.3
685	12.6
730	13.0
785	12.35
870	12.35
1350	12.60

(Continued)

Table 5. Pressure Drop Data (Continued)

Glass Beads, G. C.; Bed Weight, 500 gm

Flow Rate (cc/min)	Pressure Drop (in. of water)
1860	12.65
2230	12.75
2660	12.80

Glass Beads, G. C.; Bed Weight, 600 gm

365	8.2
640	14.15
710	15.35
750	15.85
805	14.85
970	15.00
1685	15.20
2060	15.20
2510	15.35

Glass Beads, G. D.; Bed Weight, 400 gm

130	10.35
220	13.15
250	9.7

(Continued)

Table 5. Pressure Drop Data (Continued)

Glass Beads, G. D.; Bed Weight, 400 gm

Flow Rate (cc/min)	Pressure Drop (in. of water)
320	9.35
1180	9.85
1750	9.90
2110	10.05
2450	10.10

Glass Beads, G. D.; Bed Weight, 500 gm

120	9.45
170	14.15
220	15.75
250	11.90
420	12.15
1350	12.50
1880	12.60
2140	12.60

(Continued)

Table 5. Pressure Drop Data (Continued)

Glass Beads, G. D.; Bed Weight, 600 gm

Flow Rate (cc/min)	Pressure Drop (in. of water)
120	10.65
170	17.05
220	18.40
285	14.50
1180	15.10
1860	15.10
2310	15.10

Catalyst, Silica Alumina; Bed Weight, 200 gm

90	3.6
120	5.6
130	4.55
360	4.85
1510	5.05
1960	5.05

(Continued)

Table 5. Pressure Drop Data (Concluded)

Catalyst, Silica Alumina; Bed Weight, 300 gm

Flow Rate (cc/min)	Pressure Drop (in. of water)
90	3.40
120	7.60
125	8.35
130	7.70
780	7.50
1800	7.50
2150	7.50

Polystyrene; Bed Weight, 300 gm

640	4.0
870	4.90
1185	6.10
1505	7.25
1700	8.10
2100	9.70
2300	8.20
2800	8.35

Table 6. Viscometer Data

Glass Beads, G. A.

W_b = 600 gm
f.r. = 1910 cc/min

ΔP = 14.95 in. water
L = 10.7 in.

Distance of Spindle Above Bed Bottom (inch)	Viscometer Indication at Spindle Rotation Rates (in rpm) of			
	6	12	30	60
	(Arbitrary Units)			
0.5	60	70	84	--
1	46	50	75	90
2	23	37	56	75
3	20	34	53	71
4	17	29	48	65
5	17	29	50	70
6	17	29	48	66
7	17	29	49	69
8	15	26	48	66
9	12	25	43	65

(Continued)

Table 6. Viscometer Data (Continued)

Glass Beads, G. A.

W_b = 600 gm Δp = 15.05 in. water
f.r. = 2100 cc/min   L = 10.8 in.

Distance of Spindle Above Bed Bottom (inch)	Viscometer Indication at Spindle Rotation Rates (in rpm) of			
	6	12	30	60
		(Arbitrary Units)		
0.5	49	62	75	91
1	32	48	63	80
2	15	28	53	76
3	15	27	52	74
4	15	28	51	70
5	13	28	48	72
6	13	27	50	73
7	13	27	51	73
8	13	27	49	73
9	9	21	45	71

Glass Beads, G. A.

W_b = 600 gm Δp = 15.1 in. water
f.r. = 2270 cc/min   L = 10.9 in.

0.5	35	48	62	72
1	16	32	52	61
2	12	24	42	62
3	10	23	43	62

(Continued)

Table 6. Viscometer Data (Continued)

Glass Beads, G. A.

W_b = 600 gm Δp = 15.1 <u>in</u>. water
f.r. = 2270 cc/min L = 10.9 <u>in</u>.

Distance of Spindle Above Bed Bottom (inch)	Viscometer Indication at Spindle Rotation Rates (in rpm) of			
	6	12	30	60
	(Arbitrary Units)			
4	11	23	48	72
5	15	29	54	75
6	14	25	53	76
7	14	29	53	76
8	13	27	53	75
9	11	25	53	76

Glass Beads, G. A.

W_b = 600 gm Δp = 15.1 <u>in</u>. water
f.r. = 2420 cc/min L = 11 <u>in</u>.

	6	12	30	60
0.5	30	45	59	74
1	11	23	42	62
2	10	20	42	64
3	11	22	48	68
4	13	26	54	75
5	15	28	55	80
6	15	30	56	84
7	15	31	55	82

(Continued)

Table 6. Viscometer Data (Continued)

Glass Beads, G. A.

W_b = 600 gm Δp = 15.1 in. water
f.r. = 2420 cc/min   L = 11 in.

Distance of Spindle Above Bed Bottom (inch)	Viscometer Indication at Spindle Rotation Rates (in rpm) of			
	6	12	30	60
		(Arbitrary Units)		
8	14	30	54	83
9	13	24	50	80

Glass Beads, G. A.

W_b = 500 gm Δp = 12.45 in. water
f.r. = 1910 cc/min   L = 9.0 in.

0.5	53	63	74	83
1	34	45	55	70
2	17	28	46	63
3	17	29	47	63
4	17	28	45	62
5	17	28	45	61
6	18	29	45	61
7	17	28	45	62

(Continued)

Table 6. Viscometer Data (Continued)

Glass Beads, G. A.

W_b = 500 gm
f.r. = 2100 cc/min

ΔP = 12.45 in. water
L = 9.0 in.

Distance of Spindle Above Bed Bottom (inch)	Viscometer Indication at Spindle Rotation Rates (in rpm) of			
	6	12	30	60
		(Arbitrary Units)		
0.5	48	57	69	77
1	26	34	50	71
2	16	27	44	65
3	15	26	43	63
4	15	26	45	60
5	15	26	46	61
6	16	26	46	61
7	15	29	50	63

Glass Beads, G. A.

W_b = 500 gm
f.r. = 2270 cc/min

ΔP = 12.45 in. water
L = 9.1 in.

	6	12	30	60
0.5	40	53	64	75
1	21	29	47	63
2	11	22	42	59
3	10	23	43	60
4	12	25	44	61
5	12	25	44	65
6	13	29	49	70
7	14	28	47	74

(Continued)

Table 6. Viscometer Data (Continued)

Glass Beads, G. A.

W_b = 500 gm Δp = 12.5 in. water
f.r. = 2420 cc/min   L = 9.1 in.

| Distance of Spindle Above Bed Bottom (inch) | Viscometer Indication at Spindle Rotation Rates (in rpm) of | | | |
| | 6 | 12 | 30 | 60 |
		(Arbitrary Units)		
0.5	38	53	63	74
1	13	24	41	59
2	12	21	42	60
3	12	23	43	61
4	13	27	48	67
5	14	28	48	69
6	15	28	52	72
7	13	28	53	78

Glass Beads, G. A.

W_b = 500 gm Δp = 12.5 in. water
f.r. = 2550 cc/min   L = 9.2 in.

	6	12	30	60
0.5	28	43	59	71
1	11	23	38	56
2	10	20	43	60
3	9	22	46	67
4	10	23	50	75
5	13	26	53	75
6	14	27	56	82
7	10	23	58	83

(Continued)

Table 6. Viscometer Data (Continued)

Glass Beads, G. A.

W_b = 400 gm Δp = 9.85 in. water
f.r. = 1700 cc/min   L = 7.1 in.

| Distance of Spindle Above Bed Bottom (inch) | Viscometer Indication at Spindle Rotation Rates (in rpm) of | | | |
| | 6 | 12 | 30 | 60 |
		(Arbitrary Units)		
0.5	63	75	85	96
1	44	56	67	78
2	23	37	50	65
3	19	28	45	63
4	19	29	45	63
5	16	27	43	56

Glass Beads, G. A.

W_b = 400 gm Δp = 9.9 in. water
f.r. = 1910 cc/min   L = 7.2 in.

0.5	47	55	70	80
1	29	44	53	66
2	18	30	45	64
3	18	31	50	63
4	17	29	45	62
5	14	26	41	61

(Continued)

Table 6.   Viscometer Data (Continued)

Glass Beads, G. A.

W_b = 400 gm
f.r. = 2100 cc/min

Δp = 10 in. water
L = 7.3 in.

Distance of Spindle Above Bed Bottom (inch)	Viscometer Indication at Spindle Rotation Rates (in rpm) of			
	6	12	30	60
	(Arbitrary Units)			
0.5	55	63	75	87
1	21	35	48	62
2	14	25	48	64
3	13	25	43	63
4	13	26	46	58
5	13	27	45	64

Glass Beads, G. A.

W_b = 400 gm
f.r. = 2270 cc/min

Δp = 10.1 in. water
L = 7.3 in.

0.5	43	50	63	73
1	18	31	48	67
2	11	23	45	60
3	12	24	44	62
4	13	27	47	65
5	9	26	49	68

(Continued)

Table 6. Viscometer Data (Continued)

Glass Beads, G. A.

W_b = 400 gm
f.r. = 2420 cc/min

Δp = 10.05 in. water
L = 7.3 in.

Distance of Spindle Above Bed Bottom (inch)	Viscometer Indication at Spindle Rotation Rates (in rpm) of			
	6	12	30	60
	(Arbitrary Units)			
0.5	34	47	65	75
1	15	25	43	55
2	8	18	40	59
3	12	20	43	68
4	12	27	47	67
5	10	23	52	72

Glass Beads, G. A.

W_b = 400 gm
f.r. = 2550 cc/min

Δp = 10.1 in. water
L = 7.3 in.

0.5	34	47	60	73
1	12	19	38	55
2	8	18	43	63
3	11	22	43	69
4	13	27	52	75
5	13	27	53	75

(Continued)

Table 6. Viscometer Data (Continued)

Glass Beads, G. B.

W_b = 600 gm Δp = 15 in. water
f.r. = 1430 cc/min   L = 11.4 in.

Distance of Spindle Above Bed Bottom (inch)	Viscometer Indication at Spindle Rotation Rates (in rpm) of			
	6	12	30	60
	(Arbitrary Units)			
0.5	56	63	80	90
1	34	48	59	65
2	21	32	43	61
3	20	31	44	56
4	22	32	43	59
5	24	33	48	64
6	24	34	47	65
7	24	37	48	67
8	24	38	50	65
9	25	37	51	65

Glass Beads, G. B.

W_b = 600 gm Δp = 15.1 in. water
f.r. = 1910 cc/min   L = 11.6 In.

0.5	44	53	63	72
1	19	30	43	58
2	11	23	44	59
3	14	23	43	63
4	16	30	49	73

(Continued)

Table 6. Viscometer Data (Continued)

Glass Beads, G. B.

W_b = 600 gm
f.r. = 1910 cc/min

Δp = 15.1 in. water
L = 11.6 in.

Distance of Spindle Above Bed Bottom (inch)	Viscometer Indication at Spindle Rotation Rates (in rpm) of			
	6	12	30	60
	(Arbitrary Units)			
5	18	34	56	82
6	22	37	60	83
7	22	38	63	81
8	23	40	65	81
9	23	39	67	85

Glass Beads, G. B.

W_b = 600 gm
f.r. = 2270 cc/min

Δp = 15.3 in. water
L = 11.8 in.

	6	12	30	60
0.5	36	46	57	68
1	10	18	39	57
2	8	20	43	63
3	11	39	52	65
4	15	35	58	74
5	16	38	63	85
6	20	36	77	95
7	20	42	77	97
8	18	38	83	98
9	16	35	75	99

(Continued)

Table 6. Viscometer Data (Continued)

Glass Beads, G. B.

W_b = 600 gm
f.r. = 2550 cc/min

Δp = 15.35 in. water
L = 12.0 in.

Distance of Spindle Above Bed Bottom (inch)	Viscometer Indication at Spindle Rotation Rates (in rpm) of			
	6	12	30	60
	(Arbitrary Units)			
0.5	29	35	50	63
1	6	16	42	60
2	8	22	42	65
3	12	23	48	73
4	18	31	63	93
5	15	31	72	97
6	16	36	75	98
7	18	35	79	98
8	19	36	80	100
9	15	34	76	100

Glass Beads, G. B.

W_b = 600 gm
f.r. = 3075 cc/min

Δp = 15.35 in. water
L = 12.1 in.

Distance of Spindle Above Bed Bottom (inch)	6	12	30	60
0.5	16	27	50	61
1	8	16	37	60
2	8	20	44	68
3	10	20	53	84
4	11	31	60	93

(Continued)

Table 6. Viscometer Data (Continued)

Glass Beads, G. B.

W_b = 600 gm Δp = 15.35 in. water
f.r. = 3075 cc/min   L = 12.1 in.

Distance of Spindle Above Bed Bottom (inch)	Viscometer Indication at Spindle Rotation Rates (in rpm) of			
	6	12	30	60
	(Arbitrary Units)			
5	15	34	73	97
6	15	31	75	100+
7	10	30	73	100+
8	8	28	80	100+
9	6	19	78	99

Glass Beads, G. B.

W_b = 500 gm Δp = 12.5 in. water
f.r. = 1910 cc/min   L = 9.7 in.

0.5	51	63	71	80
1	18	28	45	56
2	11	22	41	59
3	12	23	43	65
4	14	26	47	66
5	18	34	55	74
6	21	34	58	93
7	19	36	60	82

(Continued)

Table 6. Viscometer Data (Continued)

Glass Beads, G. B.

W_b = 500 gm
f.r. = 2270 cc/min

Δp = 12.7 in. water
L = 9.9 in.

Distance of Spindle Above Bed Bottom (inch)	Viscometer Indication at Spindle Rotation Rates (in rpm) of			
	6	12	30	60
	(Arbitrary Units)			
0.5	40	48	60	70
1	10	19	37	56
2	10	20	42	61
3	12	23	43	61
4	14	31	53	77
5	16	33	66	84
6	17	36	70	92
7	17	34	72	98

Glass Beads, G. B.

W_b = 500 gm
f.r. = 2550 cc/min

Δp = 12.8 in. water
L = 10.0 in.

Distance of Spindle Above Bed Bottom (inch)	6	12	30	60
0.5	24	40	50	62
1	9	19	38	60
2	10	19	42	61
3	11	22	48	74
4	13	28	56	78
5	15	31	65	90
6	17	35	68	92
7	15	33	70	97

(Continued)

Table 6. Viscometer Data (Continued)

Glass Beads, G. B.

W_b = 500 gm
f.r. = 3075 cc/min

Δp = 12.8 in. water
L = 10.05 in.

Distance of Spindle Above Bed Bottom (inch)	Viscometer Indication at Spindle Rotation Rates (in rpm) of			
	6	12	30	60
		(Arbitrary Units)		
0.5	14	21	41	60
1	8	16	36	57
2	8	17	38	67
3	10	20	50	74
4	11	24	62	92
5	15	30	73	98
6	14	30	73	98
7	15	30	70	100

Glass Beads, G. B.

W_b = 500 gm
f.r. = 3375 cc/min

Δp = 12.8 in. water
L = 10.1 in.

	6	12	30	60
0.5	8	16	36	56
1	7.5	15	36	56
2	7	14	42	66
3	11	23	50	76
4	13	26	67	92
5	14	26	63	95
6	12	25	66	100
7	13	25	64	100

(Continued)

Table 6. Viscometer Data (Continued)

Glass Beads, G. B.

W_b = 500 gm
f.r. = 1430 cc/min

Δp = 12.45 in. water
L = 9.5 in.

Distance of Spindle Above Bed Bottom (inch)	Viscometer Indication at Spindle Rotation Rates (in rpm) of			
	6	12	30	60
	(Arbitrary Units)			
0.5	68	84	87	95
1	35	47	53	72
2	22	29	43	60
3	21	29	41	58
4	23	30	43	57
5	25	32	46	60
6	27	33	49	65
7	21	33	49	61

Glass Beads, G. B.

W_b = 400 gm
f.r. = 1700 cc/min

Δp = 10 in. water
L = 7.7 in.

0.5	55	64	70	78
1	34	43	54	65
2	12	23	40	57
3	13	23	39	54
4	16	26	43	55
5	15	27	44	61

(Continued)

Table 6. **Viscometer Data** (Continued)

Glass Beads, G. B.

W_b = 400 gm
f.r. = 1910 cc/min

Δp = 10 in. water
L = 7.7 in.

Distance of Spindle Above Bed Bottom (inch)	Viscometer Indication at Spindle Rotation Rates (in rpm) of			
	6	12	30	60
		(Arbitrary Units)		
0.5	50	59	70	76
1	17	32	45	56
2	11	20	43	53
3	11	22	41	60
4	13	26	45	63
5	13	28	48	67

Glass Beads, G. B.

W_b = 400 gm
f.r. = 2270 cc/min

Δp = 10.1 in. water
L = 7.8 in.

0.5	28	40	54	62
1	9	18	40	55
2	9	18	40	58
3	11	22	44	66
4	12	24	57	77
5	14	29	61	81

(Continued)

Table 6. **Viscometer Data** (Continued)

Glass Beads, G. B.

W_b = 400 gm
f.r. = 2550 cc/min

Δp = 10.1 in. water
L = 7.9 in.

Distance of Spindle Above Bed Bottom (inch)	Viscometer Indication at Spindle Rotation Rates (in rpm) of			
	6	12	30	60
		(Arbitrary Units)		
0.5	19	33	42	62
1	9	17	35	55
2	9	18	37	62
3	10	20	45	73
4	14	27	58	82
5	14	28	63	85

Glass Beads, G. B.

W_b = 400 gm
f.r. = 3225 cc/min

Δp = 10.2 in. water
L = 8.1 in.

0.5	8	17	35	57
1	7	14	35	59
2	8	19	41	64
3	10	21	48	77
4	12	24	60	95
5	14	29	62	98

(Continued)

Table 6. Viscometer Data (Continued)

Glass Beads, G. C.

W_b = 600 gm
f.r. = 1040 cc/min

$\triangle p$ = 15 in. water
L = 11.15 in.

Distance of Spindle Above Bed Bottom (inch)	Viscometer Indication at Spindle Rotation Rates (in rpm) of			
	6	12	30	60
	(Arbitrary Units)			
0.5	68	80	87	81
1	47	53	61	61
2	27	35	44	50
3	26	40	47	50
4	28	36	41	45
5	29	41	50	52
6	31	43	53	58
7	30	38	50	59
8	32	39	45	53
9	29	45	50	58

Glass Beads, G. C.

W_b = 600 gm
f.r. = 1430 cc/min

$\triangle p$ = 15 in. water
L = 11.3 in.

0.5	58	73	74	82
1	34	50	54	61
2	21	36	46	55
3	20	31	45	53
4	26	38	58	65

(Continued)

Table 6. Viscometer Data (Continued)

Glass Beads, G. C.

W_b = 600 gm Δp = 15 in. water
f.r. = 1430 cc/min   L = 11.3 in.

Distance of Spindle Above Bed Bottom (inch)	Viscometer Indication at Spindle Rotation Rates (in rpm) of			
	6	12	30	60
		(Arbitrary Units)		
5	24	43	55	63
6	26	43	62	68
7	27	48	60	72
8	28	49	55	78
9	25	45	70	77

Glass Beads, G. C.

W_b = 600 gm Δp = 15.1 in. water
f.r. = 1910 cc/min   L = 11.4 in.

Distance of Spindle Above Bed Bottom (inch)	6	12	30	60
0.5	42	46	56	70
1	6	15	35	63
2	12	18	36	60
3	10	23	43	67
4	13	32	60	80
5	13	33	63	91
6	13	33	68	97
7	9	30	73	--
8	10	28	70	--
9	13	23	72	--

(Continued)

Table 6.   Viscometer Data (Continued)

Glass Beads, G. C.

W_b = 600 gm
f.r. = 2270 cc/min

Δp = 15.2 in. water
L = 11.5 $\underline{in}$.

Distance of Spindle Above Bed Bottom (inch)	Viscometer Indication at Spindle Rotation Rates (in rpm) of			
	6	12	30	60
	(Arbitrary Units)			
0.5	42	46	56	70
1	6	15	35	63
2	12	18	36	60
3	10	23	43	67
4	13	32	60	80
5	13	33	63	91
6	13	33	68	97
7	9	30	73	--
8	10	28	70	--
9	13	23	72	--

Glass Beads, G. C.

W_b = 600 gm
f.r. = 2550 cc/min

Δp = 15.4 in. water
L = 11.7 $\underline{in}$.

	6	12	30	60
0.5	21	32	47	63
1	6	19	35	60
2	7	19	43	62
3	11	21	48	73
4	11	27	58	83

(Continued)

Table 6. Viscometer Data (Continued)

Glass Beads, G. C.

W_b = 600 gm
f.r. = 2550 cc/min

$\triangle p$ = 15.4 in. water
L = 11.7 in.

Distance of Spindle Above Bed Bottom (inch)	Viscometer Indication at Spindle Rotation Rates (in rpm) of			
	6	12	30	60
		(Arbitrary Units)		
5	13	27	64	98
6	13	27	63	--
7	8	23	70	--
8	6	18	82	--
9	7	15	80	--

Glass Beads, G. C.

W_b = 600 gm
f.r. = 3800 cc/min

$\triangle p$ = 15.5 in. water
L = 12 in.

0.5	5	15	34	51
1	1	11	33	54
2	3	15	38	67
3	5	16	48	84
4	7	19	57	98
5	11	24	65	--
6	6	15	63	--
7	5	16	63	--
8	4	13	62	--

(Continued)

Table 6. Viscometer Data (Continued)

Glass Beads, G. C.

W_b = 500 gm
f.r. = 1090 cc/min

Δp = 12.3 in. water
L = 9.2 in.

Distance of Spindle Above Bed Bottom (inch)	Viscometer Indication at Spindle Rotation Rates (in rpm) of			
	6	12	30	60
	(Arbitrary Units)			
0.5	59	65	79	83
1	42	48	55	68
2	26	32	43	57
3	22	29	39	57
4	24	30	40	55
5	21	28	42	55
6	20	20	42	55
7	20	28	41	54

Glass Beads, G. C.

W_b = 500 gm
f.r. = 1430 cc/min

Δp = 12.4 in. water
L = 9.3 in.

0.5	52	60	75	83
1	31	42	53	65
2	12	23	41	60
3	16	23	39	56
4	18	30	47	57
5	20	33	50	63
6	23	35	53	72
7	18	33	53	69

(Continued)

Table 6. Viscometer Data (Continued)

Glass Beads, G. C.

W_b = 500 gm
f.r. = 1910 cc/min

$\triangle p$ = 12.6 in. water
L = 9.5 in.

Distance of Spindle Above Bed Bottom (inch)	Viscometer Indication at Spindle Rotation Rates (in rpm) of			
	6	12	30	60
		(Arbitrary Units)		
0.5	47	57	65	75
1	11	24	41	57
2	8	21	38	56
3	10	23	47	65
4	12	27	53	74
5	16	34	61	80
6	16	34	65	87
7	15	33	62	97

Glass Beads, G. C.

W_b = 500 gm
f.r. = 2270 cc/min

$\triangle p$ = 12.65 in. water
L = 9.6 in.

0.5	23	36	42	57
1	9	19	35	58
2	9	21	43	56
3	12	26	47	68
4	16	33	58	80
5	18	35	65	80
6	20	35	65	93
7	16	28	73	95

(Continued)

Table 6. Viscometer Data (Continued)

Glass Beads, G. C.

W_b = 500 gm
f.r. = 2550 cc/min

Δp = 12.65 in. water
L = 9.6 in.

Distance of Spindle Above Bed Bottom (inch)	Viscometer Indication at Spindle Rotation Rates (in rpm) of			
	6	12	30	60
		(Arbitrary Units)		
0.5	26	39	44	63
1	9	18	37	55
2	10	23	42	55
3	14	26	46	61
4	15	32	61	78
5	15	35	65	94
6	14	23	73	98
7	10	26	60	98

Glass Beads, G. C.

W_b = 500 gm
f.r. = 3450 cc/min

Δp = 12.7 in. water
L = 9.7 in.

0.5	9	20	38	47
1	6	15	33	54
2	10	20	43	58
3	13	25	53	74
4	11	27	63	94
5	13	2	60	95
6	10	25	65	98
7	10	20	63	--

(Continued)

Table 6. Viscometer Data (Continued)

Glass Beads, G. C.

W_b = 400 gm
f.r. = 1090 cc/min

$\triangle p$ = 9.85 in. water
L = 7.3 in.

Distance of Spindle Above Bed Bottom (inch)	Viscometer Indication at Spindle Rotation Rates (in rpm) of			
	6	12	30	60
	(Arbitrary Units)			
0.5	60	63	78	86
1	39	48	62	72
2	22	29	42	60
3	18	26	40	57
4	17	26	40	57
5	13	23	35	50
6	11	21	35	50

Glass Beads, G. C.

W_b = 400 gm
f.r. = 1430 cc/min

$\triangle p$ = 9.95 in. water
L = 7.4 in.

0.5	45	53	70	83
1	23	36	47	62
2	7	18	37	56
3	8	18	37	50
4	9	20	37	55
5	10	22	36	55
6	9	23	37	60

(Continued)

Table 6. Viscometer Data (Continued)

Glass Beads, G. C.

W_b = 400 gm
f.r. = 1910 cc/min

Δp = 10 in. water
L = 7.6 in.

Distance of Spindle Above Bed Bottom (inch)	Viscometer Indication at Spindle Rotation Rates (in rpm) of			
	6	12	30	60
		(Arbitrary Units)		
0.5	41	52	55	65
1	6	16	32	54
2	5	15	34	55
3	7	20	35	56
4	10	21	45	65
5	12	25	49	71
6	12	25	53	74

Glass Beads, G. C.

W_b = 400 gm
f.r. = 2270 cc/min

Δp = 10.1 in. water
L = 7.7 in.

0.5	27	40	46	64
1	5	16	34	57
2	4	12	34	56
3	6	17	42	65
4	9	22	51	73
5	10	23	55	81
6	9	23	62	92

(Continued)

Table 6. Viscometer Data (Continued)

Glass Beads, G. C.

W_b = 400 gm
f.r. = 2250 cc/min

Δp = 10.1 in. water
L = 7.8 in.

Distance of Spindle Above Bed Bottom (inch)	Viscometer Indication at Spindle Rotation Rates (in rpm) of			
	6	12	30	60
	(Arbitrary Units)			
0.5	17	27	46	61
1	4	11	34	56
2	6	15	35	60
3	7	18	43	70
4	10	23	52	80
5	11	23	55	85
6	10	24	65	96

Glass Beads, G. D.

W_b = 600 gm
f.r. = 660 cc/min

Δp = 14.9 in. water
L = 13.5 in.

	6	12	30	60
1	--	--	--	--
2	40	44	57	53
3	25	34	40	47
4	26	33	36	41
5	26	33	41	47
6	25	33	43	51
7	27	37	46	57
8	29	40	49	60
9	32	42	53	63
10	29	42	50	59

(Continued)

Table 6. Viscometer Data (Continued)

Glass Beads, G. D.

W_b = 600 gm
f.r. = 1430 cc/min

Δp = 15 in. water
L = 13.7 in.

| Distance of Spindle Above Bed Bottom (inch) | Viscometer Indication at Spindle Rotation Rates (in rpm) of | | | |
| | 6 | 12 | 30 | 60 |
	(Arbitrary Units)			
1	10	23	43	52
2	5	11	25	35
3	5	11	26	40
4	11	17	35	43
5	5	17	36	46
6	6	14	37	55
7	5	17	39	57
8	7	18	41	60
9	6	17	53	65
10	5	17	53	70

Glass Beads, G. D.

W_b = 600 gm
f.r. = 1910 cc/min

Δp = 14.6 in. water
L = 13.7 in.

1	7	15	31	41
2	4	22	55	80
3	5	13	36	82
4	6	12	30	50
5	4	11	31	50

(Continued)

Table 6. **V**iscometer Data (Continued)

Glass Beads, G. D.

W_b = 600 gm
f.r. = 1910 cc/min

$\triangle p$ = 14.6 in. water
L = 13.7 in.

Distance of Spindle Above Bed Bottom (inch)	Viscometer Indication at Spindle Rotation Rates (in rpm) of			
	6	12	30	60
		(Arbitrary Units)		
6	5	11	30	50
7	5	10	33	61
8	6	11	31	60
9	4	10	33	70
10	3	7	36	85

Glass Beads, G. D.

W_b = 500 gm
f.r. = 540 cc/min

$\triangle p$ = 12.2 in. water
L = 11.2 in.

1	--	--	--	--
2	32	39	45	53
3	23	27	35	41
4	21	26	35	41
5	22	28	36	42
6	22	29	41	47
7	22	30	42	47
8	21	30	43	47
9	20	30	43	47

(Continued)

Table 6. Viscometer Data (Continued)

Glass Beads, G. D.

W_b = 500 gm
f.r. = 1430 cc/min

ΔP = 12.4 in. water
L = 11.5 in.

Distance of Spindle Above Bed Bottom (inch)	Viscometer Indication at Spindle Rotation Rates (in rpm) of			
	6	12	30	60
		(Arbitrary Units)		
1	14	23	37	45
2	6	13	26	39
3	6	13	23	38
4	7	15	28	40
5	8	17	34	47
6	8	17	35	52
7	8	17	39	57
8	7	14	40	54
9	6	14	37	57

Glass Beads, G. D.

W_b = 500 gm
f.r. = 1910 cc/min

ΔP = 12.4 in. water
L = 11.4 in.

1	5	10	22	47
2	7	15	41	67
3	6	13	30	58
4	6	14	30	48
5	5	11	33	46
6	4	10	31	53

(Continued)

Table 6. Viscometer Data (Continued)

Glass Beads, G. D.

W_b = 500 gm
f.r. = 1910 cc/min

Δp = 12.4 in. water
L = 11.4 in.

Distance of Spindle Above Bed Bottom (inch)	Viscometer Indication at Spindle Rotation Rates (in rpm) of			
	6	12	30	60
	(Arbitrary Units)			
7	5	14	33	53
8	7	14	40	54
9	6	14	37	57

Glass Beads, G. D.

W_b = 500 gm
f.r. = 2270 cc/min

Δp = 12.4 in. water
L = 11.5 in.

	6	12	30	60
1	4	12	27	30
2	5	10	40	47
3	6	11	30	43
4	5	12	28	45
5	4	10	31	--
6	6	12	32	--
7	5	10	33	--
8	5	12	30	--

(Continued)

Table 6. Viscometer Data (Continued)

Glass Beads, G. D.

W_b = 400 gm
f.r. = 540 cc/min

Δp = 9.75 in. water
L = 9.2 in.

Distance of Spindle Above Bed Bottom	Viscometer Indication at Spindle Rotation Rates (in rpm) of			
	6	12	30	60
(inch)	(Arbitrary Units)			
0.5	--	--	--	--
1	--	--	--	--
2	35	50	54	57
3	18	33	40	46
4	17	23	25	35
5	14	23	25	38
6	16	25	28	42
7	15	23	34	39

Glass Beads, G. D.

W_b = 400 gm
f.r. = 1910 cc/min

Δp = 10 in. water
L = 9.2 in.

0.5	18	23	34	39
1	5	11	25	38
2	4	10	23	37
3	5	11	23	39
4	5	13	25	43
5	5	13	32	43
6	7	13	32	50
7	4	10	27	48

(Continued)

Table 6. **V**iscometer Data (Continued)

Glass Beads, G. D.

W_b = 400 gm
f.r. = 1430 cc/min

Δp = 9.9 in. water
L = 9.2 in.

Distance of Spindle Above Bed Bottom (inch)	Viscometer Indication at Spindle Rotation Rates (in rpm) of			
	6	12	30	60
		(Arbitrary Units)		
0.5	45	53	60	63
1	14	23	35	52
2	5	11	25	35
3	5	11	22	33
4	8	14	27	37
5	8	16	32	44
6	5	15	32	45
7	5	14	32	47

Glass Beads, G. D.

W_b = 400 gm
f.r. = 2270 cc/min

Δp = 10 in. water
L = 9.2 in.

Distance of Spindle Above Bed Bottom (inch)	6	12	30	60
0.5	13	16	26	31
1	3	7	15	23
2	3	7	18	41
3	6	13	28	44
4	5	13	29	43
5	3	11	28	43
6	3	11	34	53
7	2	11	32	50

(Continued)

Table 6. Viscometer Data (Continued)

Catalyst, Silica Alumina

W_b = 150 gm
f.r. = 540 cc/min

Δp = 3.7 in. water
L = 7.9 in.

Distance of Spindle Above Bed Bottom (inch)	Viscometer Indication at Spindle Rotation Rates (in rpm) of			
	6	12	30	60
	(Arbitrary Units)			
1	--	--	--	--
2	35	47	48	49
3	23	31	32	33
4	12	19	23	24
5	6.5	10	13	15
6	5.5	8	11	13

Catalyst, Silica Alumina

W_b = 150 gm
f.r. = 660 cc/min

Δp = 3.8 in. water
L = 8.6 in.

1	3	4	8	9
2	2	3	6	9
3	2	4	6	10
4	2.5	4	7	10
5	2.5	4.5	7	10
6	3	4.5	7.5	10

(Continued)

Table 6. Viscometer Data (Continued)

Catalyst, Silica Alumina

W_b = 150 gm Δp = 3.85 in. water
f.r. = 1430 cc/min   L = 8.6 in.

Distance of Spindle Above Bed Bottom (inch)	Viscometer Indication at Spindle Rotation Rates (in rpm) of			
	6	12	30	60
		(Arbitrary Units)		
1	2	3	4.5	7
2	2	3	6	8
3	2.5	3.5	6	8
4	2.5	3	6	10
5	3	4	8	11
6	3	4	8	10

Catalyst, Silica Alumina

W_b = 200 gm Δp = 4.9 in. water
f.r. = 540 cc/min   L = 11.2 in.

1	15	22	24	27
2	6	9	12	14
3	4	7	10	11
4	4	6	9	10.5
5	3.5	5	8	10
6	3.5	5	7	9.5
7	3.5	5	7	9.5
8	4	5.5	7.5	10

(Continued)

Table 6. Viscometer Data (Continued)

Catalyst, Silica Alumina

W_b = 200 gm
f.r. = 660 cc/min

Δp = 4.95 in. water
L = 11 in.

Distance of Spindle Above Bed Bottom (inch)	Viscometer Indication at Spindle Rotation Rates (in rpm) of			
	6	12	30	60
		(Arbitrary Units)		
1	6	10	14	15
2	2.5	4	9	10
3	3	5	8	10
4	3.5	4.5	8.5	13
5	3.5	5	9	13
6	3.5	5	10	14
7	4	6.5	10	13.5
8	4	6.5	10	13

Catalyst, Silica Alumina

W_b = 200 gm
f.r. = 1430 cc/min

Δp = 5.05 in. water
L = 11.1 in.

1	2.5	4	6	10
2	2.5	4	6.5	10
3	2.5	4	7	12
4	3	5	8	13
5	3	4	9.5	14
6	3	5.5	10	13
7	3	5	9	14
8	3	5	9	13

(Continued)

Table 6. Viscometer Data (Continued)

Catalyst, Silica Alumina

W_b = 200 gm Δp = 5.1 in. water
f.r. = 1910 cc/min   L = 11.1 in.

Distance of Spindle Above Bed Bottom (inch)	Viscometer Indication at Spindle Rotation Rates (in rpm) of			
	6	12	30	60
	(Arbitrary Units)			
1	2	2.5	5	8
2	2.5	4	9	12
3	3	4	12	16
4	3	5	10	13
5	3.5	5	10	13
6	3.5	5	9	13
7	3	5	9	13
8	2.5	5	10	13

Catalyst, Silica Alumina

W_b = 250 gm Δp = 6.2 in. water
f.r. = 540 cc/min   L = 13.9 in.

Distance	6	12	30	60
1	12	17	22	23
2	5.5	8.5	11	12
3	4.5	6.5	9.5	11
4	3.5	5.5	7.5	10
5	3.5	4.5	7	9
6	3.5	5	7	9.5
7	3.5	5.5	7.5	10
8	4.5	6.5	8.5	10.5

(Continued)

Table 6. Viscometer Data (Continued)

Catalyst, Silica Alumina

W_b = 250 gm
f.r. = 540 cc/min

Δp = 6.2 in. water
L = 13.9 in.

Distance of Spindle Above Bed Bottom (inch)	Viscometer Indication at Spindle Rotation Rates (in rpm) of			
	6	12	30	60
	(Arbitrary Units)			
9	4.5	6.5	8.5	10.5
10	5	6.5	8.5	10.5
11	5	7	9	11
12	5	7	9	11

Catalyst, Silica Alumina

W_b = 250 gm
f.r. = 660 cc/min

Δp = 6.2 in. water
L = 13.9 in.

1	--	--	--	--
2	4	7	10	13
3	3	5	8	10
4	3	5	8	10
5	3.5	4.5	7	12
6	3	5	8	10
7	--	--	--	--
8	4.5	6	11	13
9	4	6	10	13
10	4.5	6	10	12
11	4	6	9	12
12	--	--	--	--

(Continued)

Table 6. Viscometer Data (Continued)

Catalyst, Silica Alumina

W_b = 250 gm
$f.r.$ = 1430 cc/min

Δp = 6.3 in. water
L = 14 in.

Distance of Spindle Above Bed Bottom (inch)	Viscometer Indication at Spindle Rotation Rates (in rpm) of			
	6	12	30	60
	(Arbitrary Units)			
1	--	--	--	--
2	3	5	8	14
3	4	7	12	16
4	5	9	15	27
5	5	10	20	28
6	4	7	15	22
7	--	--	--	--
8	4	6	13	20
9	3.5	5	10	18
10	3	5	10	14
11	3	5	10	13

Catalyst, Silica Alumina

W_b = 250 gm
$f.r.$ = 1910 cc/min

Δp = 6.4 in. water
L = 14 in.

Distance of Spindle Above Bed Bottom (inch)	6	12	30	60
1	--	--	--	--
2	3	6	14	26
3	5	8	16	26
4	5	8	16	26

(Continued)

Table 6. Viscometer Data (Continued)

Catalyst, Silica Alumina

W_b = 250 gm
f.r. = 1910 cc/min

Δp = 6.4 in. water
L = 14 in.

Distance of Spindle Above Bed Bottom (inch)	Viscometer Indication at Spindle Rotation Rates (in rpm) of			
	6	12	30	60
	(Arbitrary Units)			
5	5	7	14	23
6	4	7	13	20
7	--	--	--	--
8	3	5	11	17
9	4	6	12	16
10	3	5	10	15
11	3	6	9	15

Polystyrene

W_b = 200 gm
f.r. = 5950 cc/min

Δp = 5.2 in. water
L = 8.5 in.

	6	12	30	60
0.5	42	47	50	55
1	30	37	44	51
2	26	36	42	48
3	20	27	34	45
4	20	26	33	44
5	22	28	33	46
6	19	26	30	46

(Continued)

Table 6. Viscometer Data (Continued)

Polystyrene

W_b = 200 gm Δp = 5.25 in. water
f.r. = 6775 cc/min   L = 8.7 in.

Distance of Spindle Above Bed Bottom (inch)	Viscometer Indication at Spindle Rotation Rates (in rpm) of			
	6	12	30	60
		(Arbitrary Units)		
0.5	13	20	27	34
1	12	20	27	32
2	13	21	31	42
3	12	20	36	51
4	16	25	42	58
5	15	26	45	60
6	14	28	50	60

Polystyrene

W_b = 200 gm Δp = 5.25 in. water
f.r. = 7575 cc/min   L = 8.9 in.

	6	12	30	60
0.5	13	20	27	42
1	11	20	27	41
2	7	14	30	47
3	8	16	42	54
4	12	25	41	62
5	15	28	52	70
6	11	21	47	72

(Continued)

Table 6. Viscometer Data (Continued)

Polystyrene

W_b = 300 gm
f.r. = 5950 cc/min

Δp = 7.75 in. water
L = 12.7 in.

Distance of Spindle Above Bed Bottom (inch)	Viscometer Indication at Spindle Rotation Rates (in rpm) of			
	6	12	30	60
	(Arbitrary Units)			
0.5	72	74	82	90
1	52	63	74	89
2	15	20	25	28
3	14	20	26	30
4	15	20	26	32
5	13	21	30	40
6	16	25	31	40
7	18	25	33	40
8	--	--	--	--
9	18	27	34	51
10	23	32	38	62

Polystyrene

W_b = 300 gm
f.r. = 6775 cc/min

Δp = 7.85 in. water
L = 13.0 in.

	6	12	30	60
0.5	18	30	38	56
1	15	25	31	40
2	9	18	33	45
3	11	20	35	50
4	12	23	40	55

(Continued)

Table 6.   Viscometer Data (Continued)

Polystyrene

W_b = 300 gm
f.r. = 6775 cc/min

Δp = 7.85 in. water
L = 13.0 in.

Distance of Spindle Above Bed Bottom (inch)	Viscometer Indication at Spindle Rotation Rates (in rpm) of			
	6	12	30	60
	(Arbitrary Units)			
5	12	24	44	60
6	16	32	46	57
7	23	40	60	67
8	25	43	65	78
9	25	40	60	80
10	30	52	66	80

Polystyrene

W_b = 300 gm
f.r. = 7575 cc/min

Δp = 8.0 in. water
L = 13.3 in.

Distance	6	12	30	60
0.5	6	12	23	35
1	6	11	21	33
2	8	15	28	41
3	10	21	37	50
4	10	22	42	65
5	12	25	46	72
6	13	27	53	75
7	18	36	64	83
8	18	40	75	--
9	20	39	77	--
10	20	40	76	--

(Continued)

Table 6. Viscometer Data (Continued)

Polystyrene

W_b = 400 gm
f.r. = 6775 cc/min

Δp = 10.65 in. water
L = 17.1 in.

Distance of Spindle Above Bed Bottom (inch)	Viscometer Indication at Spindle Rotation Rates (in rpm) of			
	6	12	30	60
	(Arbitrary Units)			
1	21	27	38	46
3	17	25	40	56
7	29	39	54	65
9	32	43	67	75
10	33	53	74	85
11	37	62	77	82
12	38	63	82	85
13	39	63	83	95
14	36	50	73	80
15	30	45	63	80

(Continued)

Table 6. Viscometer Data (Concluded)

Polystyrene

W_b = 400 gm
f.r. = 7575 cc/min

Δp = 10.9 in. water
L = 17.6 in.

Distance of Spindle Above Bed Bottom (inch)	Viscometer Indication at Spindle Rotation Rates (in rpm) of			
	6	12	30	60
	(Arbitrary Units)			
1	14	27	39	60
3	11	20	44	60
7	16	30	65	80
9	20	41	82	--
10	21	44	80	--
11	24	51	75	--
12	21	44	80	--
13	20	42	90	--
14	20	40	85	--
15	17	35	72	--

BIBLIOGRAPHY

Literature Cited:

1. Grohse, E. W., "Analysis of Gas-Fluidized Solid System by X-ray Absorption," Journal American Institute of Chemical Engineers 1, 358-365 (1955).

2. Bakker, P. J. and Heertjes, P. M., "Porosity Measurements in a Fluidized Bed," British Chemical Engineering, 240-246, May (1959).

3. Matheson, G. L., Herbst, W. A. and Holt, P. H., "Characteristics of Fluid-Solid Systems," Industrial and Engineering Chemistry 41, 1099-104 (1949).

4. Ohmae, T. and Furukawa, J., "Rheological Property of Fluidized Particles," Journal Chemical Society of Japan, Industrial Chemistry Section 57, 788-91 (1954).

5. Ohmae, T. and Furukawa, J., "Liquidlike Properties of Fluidized Systems," Industrial and Engineering Chemistry 50, 821-28 (1958).

6. Diekman, R. and Forsythe, Jr., W. L., "Laboratory Prediction of Flow Properties of Fluidized Solids," Industrial and Engineering Chemistry 45, 1174-177 (1953).

7. Leva, M., Grummer, M., Weintraub, M., and Pollchik, M., "Introduction to Fluidization," Chemical Engineering Progress 44, 511-20 (1948).

8. Wilhelm, R. H. and Kwauk, M., "Fluidization of Solid Particles," Chemical Engineering Progress 44, 201-18 (1948).

9. Parent, J. D., Yagol, N. and Steiner, C. S., "Fluidizing Processes," Chemical Engineering Progress 43, 429-436 (1947).

Other References:

1. Bowles, R. L., Davie, R. P. and Todd, W. D., "A Method for the Interpretation of Brookfield Viscosities," Modern Plastics 33, No. 3, 140-148 (1955).

2. Farbar, L., "Flow Characteristics of Solid-Gas Mixtures," Industrial and Engineering Chemistry 41, 1184-91 (1949).

3. Fitch, E. B., "Interpreting Rotating Spindle Viscometer Data," Industrial and Engineering Chemistry 51, 889-90 (1959).

4. Gilliland, E. R. and Mason, E. A., "Gas and Solid Mixing in Fluidized Beds," Industrial and Engineering Chemistry 41, 1191-6 (1949).

5. Hariu, O. H., and Molstad, M. C., "Pressure Drop in Vertical Tubes in Transport of Solids by Gases," Industrial and Engineering Chemistry 41, 1148-60 (1949).

6. Krieger, I. M. and Maron, S. H., "Direct Determination of the Flow Curves of Non-Newtonian Fluids," Journal of Applied Physics 23, 147-9 (1952).

7. Lewis, W. K., Gilliland, E. R. and Bauer, W. C., "Characteristics of Fluidized Particles," Industrial and Engineering Chemistry 41, 1104-17 (1949).

8. Morse, R. D., "Fluidization of Granular Solids," (Fluid Mechanics and Quality), Industrial and Engineering Chemistry 41, 1117-24 (1949).

9. Morse, R. D., "The Uniformity of Fluidization - Its Measurement and Use," Chemical Engineering Progress 47, 199-204 (1951).

10. Othmer, D. F., Fluidization, New York: Reinhold Publishing Corporation, 1-20, 1956.

11. Toomey, R. D. and Johnston, H. F., "Gaseous Fluidization of Solid Particles," Chemical Engineering Progress 48, 220-6 (1952).

12. Zenz, F. A., "Find Best Particle Size Distribution," Petroleum Refiner 36, 261-5 (1957).